# Dehydroaromatization Pathway of Propane on PtZn/$SiO_2$+ZSM-5 Bifunctional Catalyst

Che-Wei Chang[†], Hien N. Pham[‡], Ryan Alcala[‡], Abhaya K. Datye[‡], Jeffrey T. Miller*[,†]

[†]Davidson School of Chemical Engineering, Purdue University, 480 Stadium Mall Drive, West Lafayette, Indiana 47907, United States

[‡]Department of Chemical and Biological Engineering, and Center for Microengineered Materials, University of New Mexico, Albuquerque, New Mexico 87131, United States

*Corresponding author email: mill1194@purdue.edu

## Abstract

The Cyclar process was previously developed to convert propane and butane into aromatics using gallium-loaded ZSM-5 catalysts (Ga/ZSM-5). However, the BTX (benzene, toluene, xylenes) yield is limited by light gas formation, primarily methane and ethane. In this study, relative rates, and selectivity for propane conversion on two catalytic components, gallium ($Ga/Al_2O_3$) and acid ZSM-5 (H-ZSM-5) were investigated, and the results suggest that light gas was produced by propane monomolecular cracking on ZSM-5 due to the imbalance of alkane dehydrogenation and olefin conversion rates on two catalytic functions. A PtZn alloy catalyst, which has >99% propene selectivity and 100 times higher rate than Ga, was used for the dehydrogenation function. The bifunctional PtZn/$SiO_2$+H-ZSM-5 catalyst has high yields of aromatics with low selectivity to methane (<5%) at ~70% propane conversion. The results suggest light gas yield can be minimized by utilizing the PtZn alloy and lowering the monomolecular cracking rate by ZSM-5. In addition, at 5 kPa and ~65% propane conversion, the rate and selectivity of aromatics formation is around 10 times and 30% higher, respectively, on this bifunctional catalyst than ZSM-5. Aromatics formation pathway was investigated by studying the rate and selectivity of a model intermediate (cyclohexene) on ZSM-5, PtZn/$SiO_2$ and $Ga/Al_2O_3$. Benzene is formed at similar rates on $Ga/Al_2O_3$ and ZSM-5 but cracking of cyclohexene on the latter is two orders of magnitude higher than the benzene formation rate, indicating cracking of cyclic hydrocarbons leads to low aromatization rate on Ga/ZSM-5. The

benzene formation rate on the $PtZn/SiO_2$ is 200 times higher than that on ZSM-5, suggesting aromatics are formed by the metal pathway on $PtZn/SiO_2$+ZSM-5.

**KEYWORDS:** *propane dehydroaromatization, bifunctional catalyst, platinum-zinc alloy, ZSM-5, reaction pathway, Cyclar process*

## Introduction

Shale gas production in the U.S has increased the supply of light alkanes, especially methane, ethane, and propane. Particularly, ethane and propane could be converted to ethene and propene and further transformed into other higher molecular weight hydrocarbons for production of polymers, chemicals and fuels.[1] However, many of the light alkanes production sites are distributed in the remote areas distant from most chemical processing facilities at the East, West and Gulf coast regions, which requires costly transportation over long distances by a pipeline. Direct light alkane transformation into high octane gasoline blending components, including $C_3^+$ olefins, oligomers and aromatics could become an attractive option for fuels upgrading in the rest of U.S.[1]

In early studies, Csicsery has reported the dehydrocyclodimerization of $C_3$-$C_5$ alkanes over the bifunctional $Pt/Al_2O_3$ catalysts (with acid and dehydrogenation activities) and proposed a mechanism for the reactions involving alkane dehydrogenation, olefin dimerization, cracking and aromatization.[2–5] However, $Pt/Al_2O_3$ suffers from light gas formation (methane and ethane) and fast deactivation. Instead, ZSM-5 was developed at the time and widely investigated for transformation of light paraffin and the corresponding olefins to aromatics due to its activity for acid-catalyzed reactions and resistance to deactivation.[6,7] Extensive efforts have been made to understand the reaction pathways of light alkane conversion over the ZSM-5 catalysts.[8–12] Gusinet et al. discussed the mechanism of alkane activation and the reaction scheme of $C_2$-$C_4$ alkanes aromatization on ZSM-5.[13] Due to complexity of reaction networks, reaction pathways

are mostly established based on the observed product distribution. For example, the primary products of propane on ZSM-5 are methane and ethene in equal molar amounts as well as propene and hydrogen at high temperature, which cannot be explained by typical bimolecular cracking mechanism. Instead, Haag and Dessau reported the monomolecular cracking pathway for activation of alkanes, through which pentacoordinated carbonium ions are formed which crack the feed to give hydrogen, alkanes and olefins.[14] Although it is generally accepted that the activation of alkanes might proceed via both the bimolecular hydride transfer and monomolecular cracking pathway over the ZSM-5, it is inferred that the monomolecular pathway dominates when olefin concentration becomes low and might account for formation of methane.[15,16] Gnep et al. have compared the conversion of propane and propene over ZSM-5 and concluded alkane dehydrogenation is the rate-limiting step in the conversion to aromatics.[13]

To enhance the rate of light alkane transformation, metals with dehydrogenation activity (i.e. Pt, Zn, Ga) were utilized as promoters with HZSM-5 for light alkane conversion.[17–23] Gnep et al. have investigated the product distribution on Pt/ZSM-5 and ZSM-5 for catalytic conversion of propane and propene to aromatics.[24] The distinct difference in the product yield suggested that propane aromatization occurred through a bifunctional process. Introduction of Pt enhanced not only propane dehydrogenation but also the propene aromatization process. Unfortunately, light gas formation and fast deactivation make Pt/ZSM-5 impractical for industrial purposes. Although Pt has the highest dehydrogenation activity, Zn and Ga containing ZSM-5 give higher selectivity to aromatics for propane conversion possibly due to high dehydrogenation rates of alkanes and cycloalkanes and display higher stability than Pt.[17–23] Particularly, Ga/ZSM-5 catalysts have been reported to produce the highest yield to aromatics among all the metal-promoted ZSM-5 catalysts.[25–31] Previously, Ga/ZSM-5 was utilized in the Cyclar process to convert propane and butane directly to BTX in a single reactor

at high temperature (500-600℃) and atmosphere pressure.[32,33] With promotion by Ga, the yield of aromatics in the Cyclar process can reach 60-65%. There has been significant interest in investigating the catalytic function of Ga in the aromatization of light alkanes especially propane over the Ga/HMFI catalysts. Kitagawa et al. discussed the modification of gallium loading to the mechanistic pathway of propane over ZSM-5 and concluded that Ga species do not directly participate in the activation of propane, but provide for the efficient transformation of the olefin intermediate species into aromatic hydrocarbons.[10] In contrast, Gnep et al. studied the product distribution as a function of propane conversion over Ga/ZSM-5, and concluded that Ga species might be responsible for alkane to olefin, olefin to diene, cycloalkane to cycloalkene to aromatics.[34] Although it is believed that a synergic effect exists over the bifunctional catalyst, the detailed nature of the bifunctional pathways remains uncertain.

Unfortunately, the Cyclar process is limited by low liquid yield. The yield of less than 60% aromatics reported in literatures is limited by concurrent formation of light gas, particularly methane and ethane, which can't be further transformed into BTX. Although several potential pathways for light gas formation in the dehydroaromatization process were proposed, including alkane monomolecular cracking, hydrogenolysis and aromatic dealkylation,[35,36] the most problematic reaction pathway has never been explicitly identified. In addition, catalysts with improved liquid yield have not been reported. One of the goals in this work is to determine the light gas formation pathway in the conversion of propane dehydroaromatization and develop a strategy to minimize the light gas selectivity, thus, increasing the aromatic yields. Here we report improved aromatics selectivity for the conversion of propane to gasoline-blending hydrocarbons using a bifunctional PtZn alloy-containing ZSM-5 catalyst. The product distribution was determined at different propane conversions and ratios of ZSM-5 to PtZn/$SiO_2$ to identify the individual role of two catalytic functions in the reaction pathway of propane conversion. This work shows how these factors are associated with controlling selectivity to

light gas and aromatics. In addition, reaction pathways of cyclic hydrocarbons (cyclohexene) are studied to understand the differences in the aromatization pathway of MFI, Ga/MFI and PtZn alloy-MFI catalysts.

## Experimental Section

### Catalyst Synthesis

*PtZn/$SiO_2$*

Strong electrostatic adsorption method (SEA) was firstly used on 5 g of commercially available silica (Sigma- Aldrich, Davisil Grade 646) to prepare $Zn/SiO_2$.[37] 0.68g $Zn(NO_3)_2 \cdot 6H_2O$ (Sigma-Aldrich) was dissolved in 50 mL deionized water (DI water) to obtain 3% Zn weight loading assuming all the Zn was loaded onto $SiO_2$. Subsequently, ammonium hydroxide ($NH_4OH$, Sigma-Aldrich) was added to $Zn(NO_3)_2$ solution to adjust to pH to 11-12. The $SiO_2$ was added to the Zn solution and stirred for 10 minutes. The sample was vacuum filtered and washed with 50 mL DI water for three times. The wet powder was dried overnight at 125℃ and calcined at 300℃ for 3 h (10℃ /min).

Pt was then added to the $Zn/SiO_2$ by pH adjusted incipient wetness impregnation method (IWI) to give 2% Pt weight loading in the final $PtZn/SiO_2$ catalyst. Its impregnation volume was calculated to be 1.16 mL/g by adding $H_2O$ dropwise to 1g of $SiO_2$ until it was saturated. 0.2g $Pt(NH_3)_4(NO_3)_2$ (Sigma-Aldrich) was dissolved in about 2mL DI water. 1 mL $NH_4OH$ was added to Pt solution and stirred until all crystals dissolved and the pH of the Pt solution was about 11-12. Additional DI water was added to the solution to bring the overall volume to impregnation volume of $SiO_2$. The solution was added dropwise to the $Zn/SiO_2$ support. The catalyst was dried overnight at 125℃, calcined at 200℃ for 3 h (5℃ /min ramp) and reduced at 225 °C in 5 % $H_2/N_2$ at 100 $cm^3$/min for 30 min.[38]

*$Ga/Al_2O_3$*

$Ga/Al_2O_3$ was prepared by IWI method on 5g of γ-$Al_2O_3$ (Alfa Aesar). 0.41g of citric acid (Sigma-Aldrich) was added to 1.5g of $Ga(NO_3)_3$ solution (Alfa Aesar, 9-10 wt% Ga) to obtain 3% Ga weight loading assuming all Ga was loaded onto the support. Concentrated $NH_4OH$ was added to the solution to adjust to a pH of 11-12. The solution was then diluted with DI water up to the impregnation volume and added dropwise onto $Al_2O_3$. The pre-catalyst was dried overnight at 125 °C and calcined at 550 °C for 3 h (10℃ /min).

*$PtZn/SiO_2$+ZSM-5 bifunctional catalysts*

Commercial ZSM-5 extrudes (CBV5524G, 80wt% zeolite and 20wt% alumina binder, $SiO_2/Al_2O_3$=50) were obtained from Zeolyst Inc. The ZSM-5 extrudes were firstly ground, pelleted, and sieved to retain 180-400 μm particle size and then calcined in air at 550℃ for 3h to obtain its acidic form, which will be referred as ZSM-5 catalysts. The bifunctional catalysts were prepared by physical mixing of $PtZn/SiO_2$ and ZSM-5 and referred as $PtZn/SiO_2$+ZSM-5 catalysts. The Z/PA ratio in the latter context will be defined as the weight loading ratio of ZSM-5 (Z) and $PtZn/SiO_2$ (PA).

**Catalytic Performance Test**

The catalytic performance was evaluated in a quartz tube fixed bed reactor (10.5 mm i.d.) equipped with mass flow rate controllers (Parker Porter, CM400) for atmospheric pressure conditions. A furnace (Applied Test Systems series 3210) was connected to a temperature controller to supply the heat and maintain the desired temperature. The gases used in this work are dilute (5%) and pure (99.99%) $C_3H_8$ (Indiana Oxygen), 3% $C_3H_6$ (Indiana Oxygen). The cyclohexene vapor is supplied by purging ultra-high purity $N_2$ (99.99%, Indiana Oxygen) into

cyclohexene solution (Sigma-Aldrich, 99%) through a bubbler (Ace Glass), which is maintained at 0°C with ice bath in a Dewar flask.

The catalysts were supported on quartz wool with a K-type thermocouple placed in the center bottom of the catalyst bed to monitor the temperature in the bed. Reactor effluent was discharged through a line heated to 170°C using heating tapes (Omega) and wrapped woth insulation and introduced to a gas chromatograph (Agilent 7890A) equipped with a flame ionization detector (Agilent J&W HP-AL/S column, 0.320 mm i.d. × 25m) for reactant and product quantification. $PtZn/SiO_2$ and $PtZn/SiO_2$+ZSM-5 catalysts were pretreated with $N_2$ for 15 min to remove any adsorbed moisture and reduced in 5% $H_2/N_2$ (Indiana Oxygen) at 550°C for 30 min before the reaction was performed, while $Ga/Al_2O_3$ and ZSM-5 were only pretreated with $N_2$ at 550°C for 30 min. The catalytic performances were evaluated at 550°C and atmospheric pressure. Fresh catalysts were loaded for each experiment. The conversion and product selectivity were obtained at different space velocities. Catalysts showed minor deactivation over about 5 h. As an example, propane conversion as a function of time on stream over the $PtZn/SiO_2$+ZSM-5 catalyst (Z/PA=1) is shown in Figure S1.

**X-ray Absorption Spectroscopy (XAS)**

*In situ* XAS experiments were performed at the 10-BM-B beamline at the APS for the Pt L3 edge (11.564 keV) and Ga K edge (10.375 keV) to correlate the catalytic performance with the structure information on the $PtZn/SiO_2$ and $Ga/Al_2O_3$. Samples were loaded in a six-shooter, placed in the middle of a glass tube sealed with leak-tight end caps, The $PtZn/SiO_2$ catalyst was reduced in 5% $H_2/N_2$ at 550°C and cooled in He. The measurement for the $PtZn/SiO_2$ was accompanied by a Pt foil scan which was obtained through a third ion chamber and used for calibration. The as-synthesized $Ga/Al_2O_3$ catalyst and gallium acetylacetonate ($Ga(AcAc)_3$) reference were scanned in air at room temperature. The X-ray absorption near edge structure

(XANES) spectra were used to identify the chemical state and valence of Pt or Ga, while extended X-ray absorption fine structure (EXAFS) provided information of coordination number (CN) and bond distacne (R). XANES and EXAFS data were obtained and interpreted using WinXAS v 3.1 software.[39] Feff6 calculations were performed using $Pt_1Zn_1$ phase ($R_{Pt-Zn}$=2.66, $CN_{Pt-Zn}$=8, $R_{Pt-Pt}$=2.85, $CN_{Pt-Pt}$=6). The final EXAFS fit was performed based on the fitting of calculated Pt−Zn and Pt−Pt scattering of the $Pt_1Zn_1$ structure to determine the coordination number and bond distance on the $PtZn/SiO_2$.[40] The coordination number and bond distance of $Ga/Al_2O_3$ was determined for Ga-O scattering based on experimental obtained $Ga(AcAc)_3$ spectra ($R_{Ga-O}$=1.95 Å, $CN_{Ga-O}$=6).

**Transmission Electron Microscope (TEM)**

Samples were dispersed in ethanol and mounted on holey carbon grids for examination in a JEOL NEOARM 200CF transmission electron microscope equipped with spherical aberration correction to allow atomic resolution imaging, and an Oxford Aztec Energy Dispersive System (EDS) for elemental analysis. The microscope is equipped with two large area JEOL EDS detectors for higher throughput in acquisition of x-ray fluorescence signals. Images were recorded in annular dark field (ADF) mode.

**Results and Discussion**

**Light gas formation in $Ga/Al_2O_3$+ZSM-5**

Two catalytic components, $Ga/Al_2O_3$ and ZSM-5, were investigated for their individual contribution to light gas formation for the propane dehydroaromatization process. The structure of $Ga/Al_2O_3$ catalyst characterized by *in situ* XAS is reported in Figure 1. Figure 1a shows that the XANES energy of the $Ga(AcAc)_3$ reference and $Ga/Al_2O_3$ is 10.377 keV and 10.375 keV, respectively, which is consistent with 6-coordinate octahedral $Ga^{3+}$ and 4-coordinate $Ga^{3+}$

reported in prior studies.[41–43] The EXAFS spectra were fitted to determine the coordination number and bond distance of the catalysts. The lower intensity of first shell Ga-O scattering of $Ga/Al_2O_3$ compared with that of $Ga(AcAc)_3$ is suggestive of lower coordination (Figure 1b). Table 1 shows the $k^2$-weighted EXAFS fitting parameters. The $Ga(AcAc)_3$ reference compound has a coordination number of 6 and a bond distance (Ga-O) of 1.95 Å, while $Ga/Al_2O_3$ has a coordination number of 4.2 and a bond distance of 1.85 Å. 4-coordinate $Ga^{3+}$ has a lower XANES energy by 2 eV and a shorter bond distance than 6-coordinate $Ga^{3+}$ by about 0.1 Å. The results indicate the active site is a single-site, 4-coordinate $Ga^{3+}$ ion on alumina. Similar XANES and EXAFS have been reported for $Ga/SiO_2$ propane dehydrogenation catalysts.[41,42]

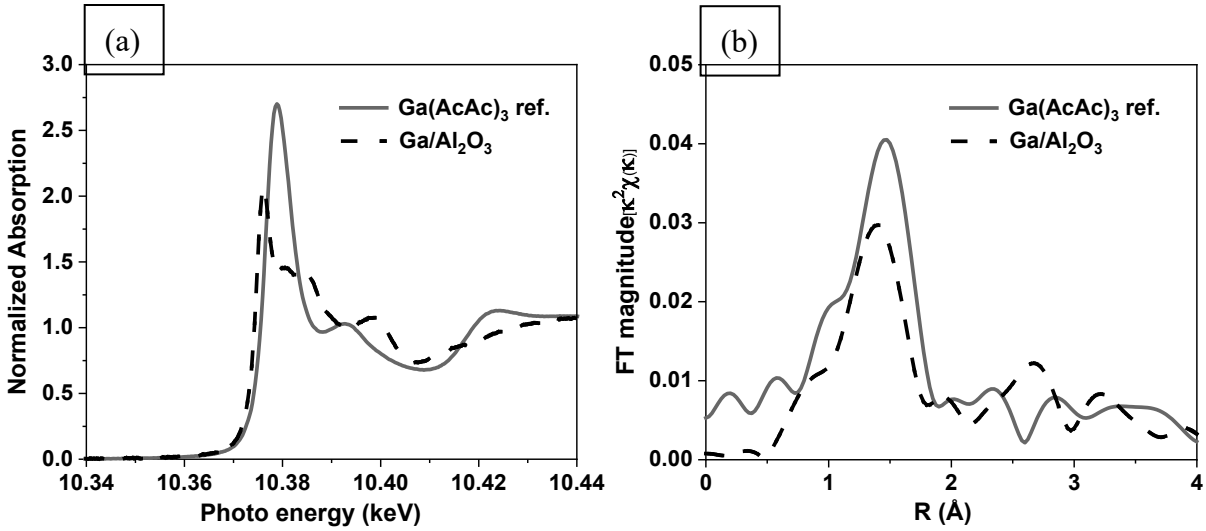


Figure 1. (a) XANES and (b) EXAFS of $Ga(AcAc)_3$ (solid) and $Ga/Al_2O_3$ (dash)

Table 1. Coordination number and bond distance from in situ EXAFS simulation of $Ga/Al_2O_3$ and $Ga(AcAc)_3$

| Sample | XANES energy (keV) | Coordination Number | Bond Distance (Å) | $\Delta\sigma^2$ |
|---|---|---|---|---|
| $Ga(AcAc)_3$ ref. | 10.377 | 6.0 | 1.95 | 0.005 |
| $Ga/Al_2O_3$ | 10.375 | 4.2 | 1.85 | 0.003 |

***propane conversion over ZSM-5 and 3% $Ga/Al_2O_3$***

The product selectivity of 5% propane at 550°C over $Ga/Al_2O_3$ and ZSM-5 is shown in Table 2. The carbon selectivity to methane is approximately 26% on the ZSM-5. At 44.4% propane

conversion, the selectivities to methane, ethane and ethene are 26.0%, 3.3% and 40.4%, indicating most of light gas are methane and ethene. Propene and higher molecular weight hydrocarbons, including butanes, butenes, $C_5^+$ oligomers and aromatics, are also formed on the ZSM-5. $Ga/Al_2O_3$ demonstrates 0.5% selectivity to methane and 0.2 % selectivity to ethane at 20.0% propane conversion. The propene selectivity is 89.7%, showing that it is moderately selective for propane dehydrogenation. However, 3.9% ethene and 5.7% butenes are also observed in the products, which are likely formed by the secondary reactions of propene.[13,34] The light gas selectivity is 3.3% (1.4% methane, 1.9% ethane) at 42.9% propane conversion. As the propane conversion increases, the propene selectivity decreases to 81.6%; while the selectivity to ethene and butenes increases to 7.5% and 7.6%, respectively, which further implies that decreasing propene selectivity is attributed to the secondary reactions.

Table 2. Propane conversion on ZSM-5 and $Ga/Al_2O_3$.

| | ZSM-5 | | 3% $Ga/Al_2O_3$ | |
|---|---|---|---|---|
| Conversion (%) | 21.8 | 44.4 | 20.0 | 42.9 |
| WHSV ($h^{-1}$) | 0.72 | 0.36 | 0.60 | 0.22 |
| Selectivity (%) | | | | |
| Methane | 25.5 | 26.0 | 0.5 | 1.4 |
| Ethane | 2.5 | 3.3 | 0.2 | 1.9 |
| Ethene | 45.6 | 40.4 | 3.9 | 7.5 |
| Propene | 18.7 | 16.8 | 89.7 | 81.6 |
| Butanes, butenes | 2.7 | 3.0 | 5.7 | 7.6 |
| $C_5^+$ paraffins, olefins and aromatics | 5.0 | 10.5 | trace[a] | trace[a] |
| Propane conversion rate ((mol $C_3$)(g catalyst) $^{-1}s^{-1}$) | $3.0\times10^{-6}$ | $3.0\times10^{-6}$ | $2.3\times10^{-6}$ | $1.9\times10^{-6}$ |
| Methane formation rate ((mol $C_1$)(g catalyst) $^{-1}s^{-1}$) | $7.7\times10^{-7}$ | $7.8\times10^{-7}$ | $1.2\times10^{-8}$ | $2.7\times10^{-8}$ |
| Ethene formation rate ((mol $C_2^=$)(g catalyst) $^{-1}s^{-1}$) | $1.4\times10^{-6}$ | $1.2\times10^{-6}$ | $9.0\times10^{-8}$ | $1.4\times10^{-7}$ |
| Propene formation rate ((mol $C_3^=$)(g catalyst) $^{-1}s^{-1}$) | $5.6\times10^{-7}$ | $5.0\times10^{-7}$ | $2.0\times10^{-6}$ | $1.6\times10^{-6}$ |

Reaction conditions: temperature, 550°C, pressure, 101 kPa, 5% $C_3H_8/N_2$

[a] Trace indicates <0.1% selectivity

The rates on each catalyst are estimated based to the carbon number of reactants consumed or products generated per gram of the catalyst (Table 2). For example, the methane formation rates are estimated by multiplying propane conversion rate and methane selectivity. The average rates at different propane conversions on two catalysts in Table 2 were utilized for comparison. Although 3% $Ga/Al_2O_3$ has higher olefin selectivity than that on ZSM-5, the average propane conversion rates on ZSM-5 ($3.0\times10^{-6}$ (mol $C_3H_8$)(g ZSM-5)$^{-1}s^{-1}$) are about 1.5 times higher than on the $Ga/Al_2O_3$ ($2.1\times10^{-6}$ (mol $C_3H_8$)(g $Ga/Al_2O_3$)$^{-1}s^{-1}$). As a result, the methane formation rates on ZSM-5 ($7.8\times10^{-7}$ (mol $CH_4$)(g ZSM-5)$^{-1}s^{-1}$) are around 40 times higher than on $Ga/Al_2O_3$ ($2.0\times10^{-8}$ (mol $CH_4$)(g $Ga/Al_2O_3$)$^{-1}s^{-1}$). The ethene formation rates on ZSM-5 ($1.3\times10^{-6}$ (mol $C_2H_4$)(g ZSM-5)$^{-1}s^{-1}$) are around 10 times higher than on $Ga/Al_2O_3$ ($1.2\times10^{-7}$(mol $C_2H_4$)(g $Ga/Al_2O_3$)$^{-1}s^{-1}$). Due to high dehydrogenation rates of Ga, the propene formation rates on the $Ga/Al_2O_3$ ($1.8\times10^{-6}$(mol $C_3H_6$)(g $Ga/Al_2O_3$)$^{-1}s^{-1}$) are 3.5 times higher than on ZSM-5 ( $5.3\times10^{-7}$ (mol $C_3H_6$)(g ZSM-5)$^{-1}s^{-1}$). The results indicate that propane conversion occurs at similar rates on ZSM-5 and $Ga/Al_2O_3$. The former makes methane and ethene on Brønsted acid sites by monomolecular cracking, while the latter makes propene by dehydrogenation. Subsequently, low molecular weight olefins (light olefins) are transformed into higher molecular weight hydrocarbons over ZSM-5; while methane remains unreactive.

***propene conversion over ZSM-5***

Propene, as one of primary olefins produced by propane, was chosen as the representative olefin to demonstrate the selectivity and rate for olefin conversion over ZSM-5 using 3% propene at 550℃.

Figure 2a shows the propene conversion rate as a function of propene conversion over ZSM-5. The propene rates are also compared to the propane conversion rates at the same temperature to understand the difference in rate and product selectivity between alkanes and olefins on the

acid sites. The average propene conversion rate is $7.2\times10^{-5}$ (mol $C_3H_6$)(g ZSM-5)$^{-1}s^{-1}$, higher than the propane conversion rate ($3.6\times10^{-6}$(mol $C_3H_8$)(g ZSM-5)$^{-1}s^{-1}$)) by a factor of about 20, indicating olefins are significantly more reactive than alkanes.[13,44] Figure 2b shows that the product distribution of propene conversion is composed of primarily ethene, $C_3$-$C_6^+$ hydrocarbons and BTX with low methane selectivity at high propene conversion (74%). Methane selectivity remains less than 1% at 20% and 32% propene conversion and increases to 4% (methane 3%, ethane 1%) at 74% conversion. At 20% propene conversion, major products are ethene (38%) and butenes (41%); while small amount of $C_5^+$ hydrocarbons (9%) and BTX (6%) are also observed.

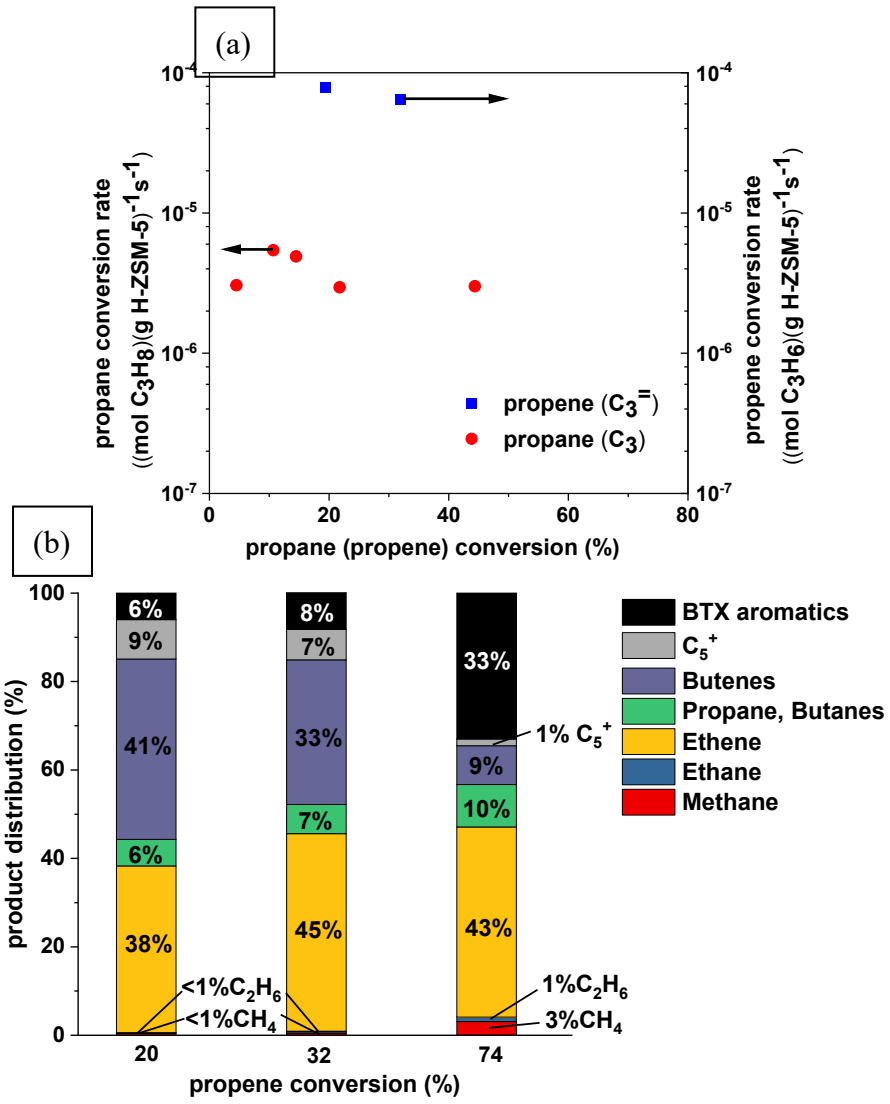


Figure 2. (a) the rates of propane[a] and propene[b] conversion (b) product distribution of propene conversion over

ZSM-5. Reaction conditions: temperature, 550 °C, pressure, 101 kPa

[a] cat., 0.1-0.5 g; 5% $C_3H_8/N_2$; WHSV=0.2-4 $h^{-1}$

[b] cat., 0.005-0.1 g; 3% $C_3H_6/N_2$; WHSV=1-20 $h^{-1}$

Generally, formation of ethene by the cracking reaction is less favored because of the stability of primary carbenium ions. However, it has previously been suggested that due to the small pore size of ZSM-5, steric confinement between the zeolite surface and adsorbed carbenium ions could stabilize the primary carbenium intermediates and likely facilitate ethene formation.[45–47] This may explain why high ethene selectivity is observed in the product mixture for propene conversion on ZSM-5 catalysts. As propene increases from 20% to 74%, the butenes and $C_5^+$ hydrocarbons decrease to 9% and 1%, respectively; while the BTX selectivity increases significantly to 33%, suggesting butenes and $C_5^+$ oligomers are formed by propene as intermediates and eventually converted to aromatics on ZSM-5 as proposed in the previous studies.[8–12] Meanwhile, the selectivity to propane and butanes increases from 6% to 10%, which is believed to form along with aromatics.[48] The ethene selectivity is highest (45%) at the intermediate conversions (32%), implying that it is generated from propene at low propene conversion and slowly converted to higher molecular weight olefins at high propene conversion. The detailed product selectivity is shown in Table S1. These results are consistent with other studies for propene conversion on MFI catalysts.[13,34]

**Structure characterization and catalytic performance and of $PtZn/SiO_2$**

PtZn intermetallic alloy was reported to be nearly 100% selective to ethene with a high rate for ethane conversion.[40] As a result, the PtZn alloy was utilized as a high activity dehydrogenation function in the bifunctional catalyst for propane conversion. The structure of the synthesized $PtZn/SiO_2$ catalyst was characterized by *in situ* XAS to ensure the formation of the PtZn alloy. Figure 3a shows the normalized absorption as a function of energy from 11.540 to 11.600 keV

on Pt foil, $Pt/SiO_2$ and $PtZn/SiO_2$. Comparing the XANES of $Pt/SiO_2$ and $PtZn/SiO_2$ catalyst with the Pt foil standard at Pt $L_3$ edge, the edge energy of Pt catalyst is 11.5640 keV, same as Pt foil. The change in the shape of the XANES of $Pt/SiO_2$ is attributed to small particle size.[49] The XANES of the $PtZn/SiO_2$ is slightly different from Pt foil and increases by 0.9 eV because of the formation of PtZn intermetallic nanoparticles.[40] Figure 3b shows the magnitude of the $k^2$-weighted FT plot. The three peaks of $Pt/SiO_2$ are characteristic peaks of metallic Pt, which has the similar shape to that of Pt foil. However, $PtZn/SiO_2$ is significantly different from metallic Pt, which suggests a PtZn intermetallic alloy was formed.

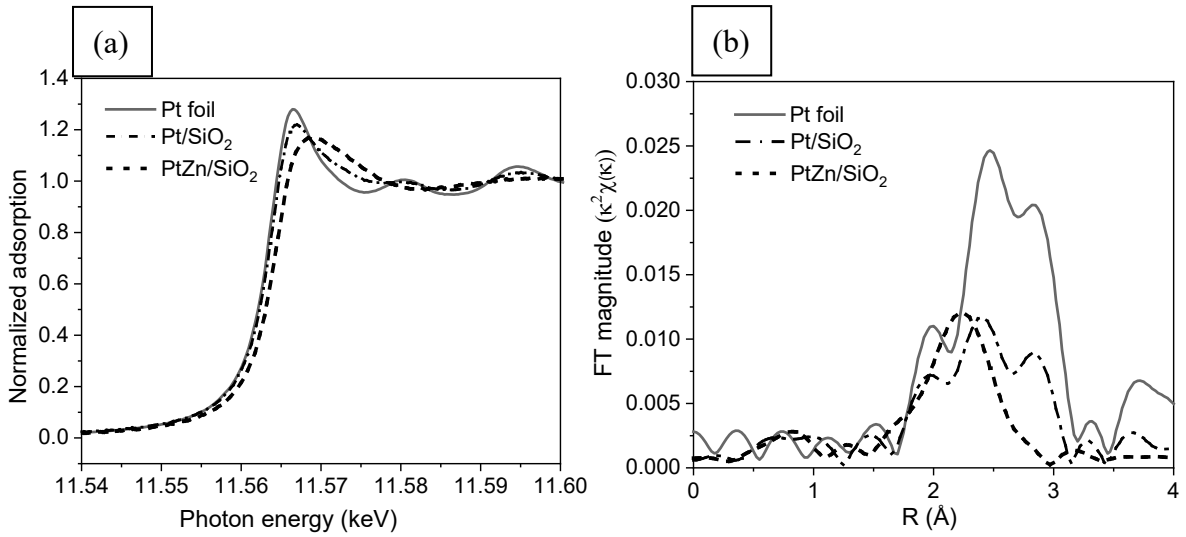


Figure 3. (a) XANES and (b) EXAFS of Pt foil (solid), $Pt/SiO_2$ (dash dot) and $PtZn/SiO_2$ (dash)

*Samples were pre-treated with 5% $H_2/N_2$ at 550°C for 1 hr and purged with He when cooling to room temperature before scanned

The $k^2$-weighted EXAFS at Pt edge of all samples was fitted to acquire the average coordination number and bond distance between Pt and the nearest neighbor atoms (Table 3). Pt-Pt with an average bond distance of 2.73 Å and coordination number of 8.6 was confirmed on $Pt/SiO_2$. On the $PtZn/SiO_2$, the average Pt-Zn bond distance of 2.56 Å with coordination number of 3.1 and average Pt-Pt bond distance of 2.71 Å with coordination number of 2.4 were obtained. The coordination number of Pt-Zn to Pt-Pt on the $PtZn/SiO_2$ is approximately 1.3, which is consistent with the $Pt_1Zn_1$ phase with a tetragonal AuCu structure.[40] In comparison to

bulk Pt and $Pt_1Zn_1$, the coordination number of both samples are smaller, implying small particles are formed. The bond distance of Pt-Zn and Pt-Pt is ~0.1 Å smaller than those reported for $Pt_1Zn_1$ phase, which can be attributed to lattice contraction as the particle size decreases.[49] The result of structure characterization is indicative of the formation of the $Pt_1Zn_1$ alloy with small particle size.

Table 3. Coordination number and bond distance from *in situ* EXAFS simulation of $Pt/SiO_2$ and $PtZn/SiO_2$

| **Sample** | **XANES energy (keV)** | **Scattering Pair** | **Coordination Number** | **Bond Distance (Å)** | **$\Delta\sigma^2$** |
|---|---|---|---|---|---|
| $Pt/SiO_2$ | 11.5640 | Pt-Pt | 8.6 | 2.73 | 0.007 |
| $PtZn/SiO_2$ | 11.5649 | Pt-Zn | 3.1 | 2.56 | 0.007 |
| | | Pt-Pt | 2.4 | 2.71 | 0.007 |

Figure 4 shows AC-STEM images of the pre-reduced $PtZn/SiO_2$ catalyst and the corresponding particle size distribution with an average particle size of 4.7 ± 3.0 nm. EDS elemental mapping was done to show the alloying of PtZn particles. Figure 5 shows elemental maps of Si $K\alpha_1$, O $K\alpha_1$, Zn $K\alpha_1$, and Pt $M\alpha_1$ corresponding to the AC-STEM image. The maps show that the particles are rich in Pt, with Zn co-existing with Pt in the particles and on the silica support. The weight ratio of Pt:Zn is close to 1:1, with excess Zn in the sample. Figure 6b and 6c show another elemental mapping of Pt $M\alpha_1$ and Zn $K\alpha_1$ corresponding to a portion of the AC-STEM image (Figure 6a). The two regions from the Pt map were then extracted to obtain the compositions. Results show that the particles contain Pt and Zn, whereas the region devoid of particles contains only Zn on the silica support. The EDS map suggests that Pt is also present in the region devoid of any particles, but the signal is at the background noise level, hence we concluded that while Zn is dispersed on the support, the Pt is only present in the form of particles.

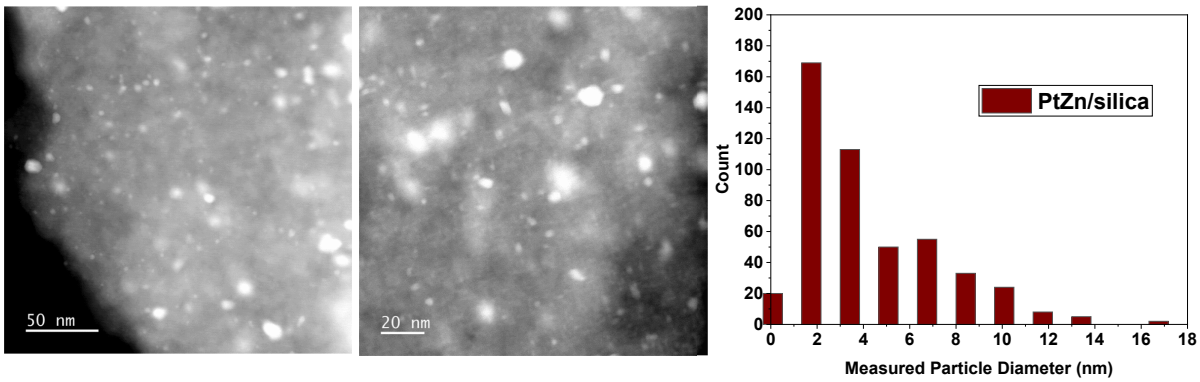


Figure 4. AC-STEM images of $PtZn/SiO_2$ pre-reduced in $H_2$, and the corresponding particle size distribution.

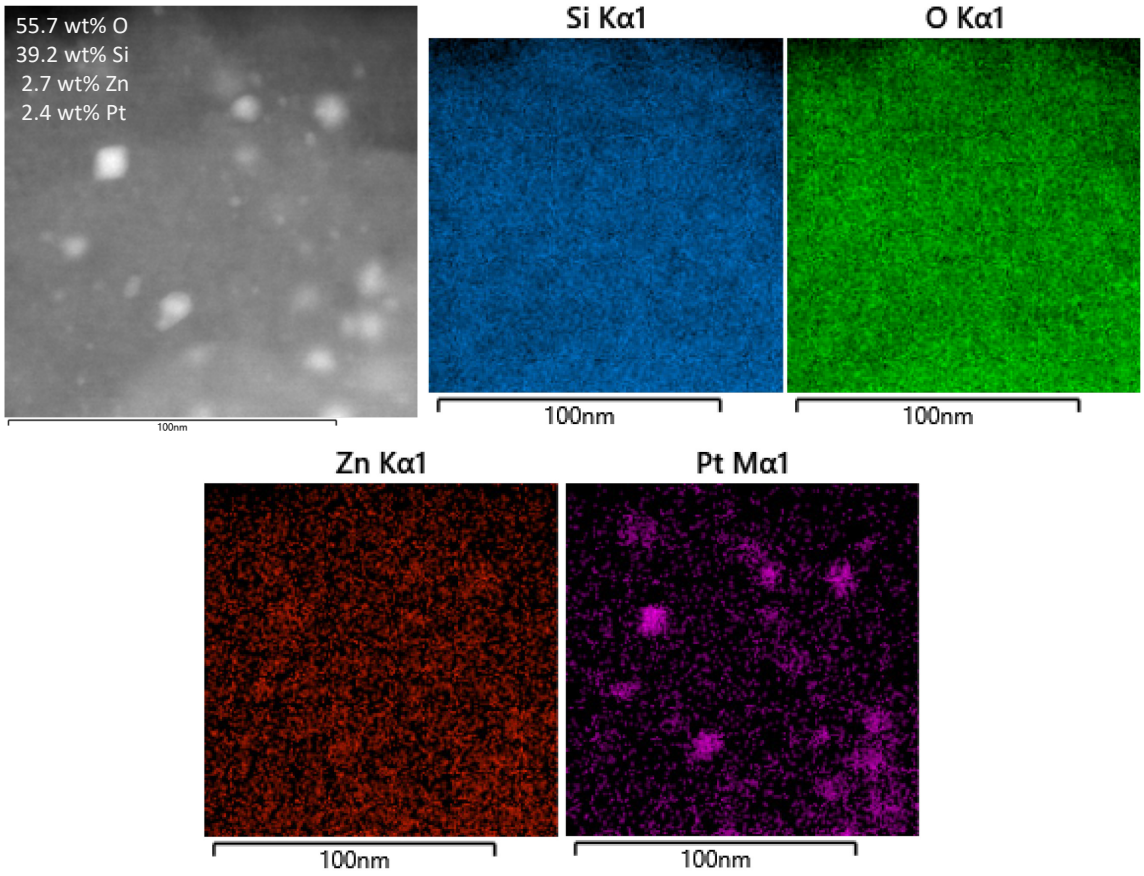


Figure 5. EDS elemental maps of Si $K\alpha_1$, O $K\alpha_1$, Zn $K\alpha_1$, and Pt $M\alpha_1$ corresponding to the AC-STEM image.

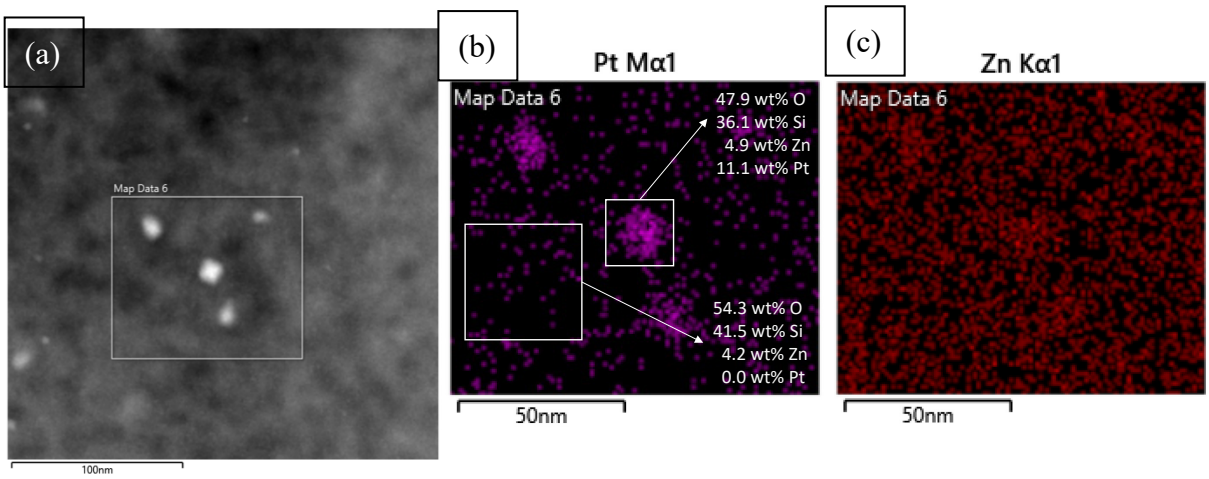


Figure 6. (a) AC-STEM image of Pt-Zn/SiO2 catalyst and EDS elemental maps of (b) Pt $M\alpha_1$ and (c) Zn $K\alpha_1$ corresponding to the region shown in the AC-STEM image (a). The two regions indicated in the white box were analyzed obtain compositions.

The catalytic performance of $PtZn/SiO_2$ was evaluated for propane dehydrogenation to estimate propane conversion rate and propene selectivity in comparison with $Ga/Al_2O_3$. Figure 7a and 7b show propene selectivity and propane conversion rates as a function of propane conversion, respectively, using 2.5% propane with 2.5% $H_2$ at 550 °C and atmosphere pressure over $PtZn/SiO_2$ and $Ga/Al_2O_3$. The purpose of cofeeding $H_2$ is to evaluate the extent of hydrogenolysis on each catalyst. $PtZn/SiO_2$ can achieve nearly 100% selectivity to propene within 10-55% propane conversion even with hydrogen, which suggests that methane formation by hydrogenolysis is nearly suppressed on the $PtZn/SiO_2$. $Ga/Al_2O_3$ has demonstrated 78-88% selectivity to propene and 5-13% selectivity to methane and ethane within 18-40% propane conversion, suggesting that hydrogenolysis can be a contributor to light gas formation at high propane conversion with Ga-MFI catalysts. The propane conversion rates on $PtZn/SiO_2$ ($2.5\times10^{-5}$ (mol $C_3H_8$)(g $PtZn/SiO_2$)$^{-1}s^{-1}$) are 25 times higher than on $Ga/Al_2O_3$ ( $9.8\times10^{-7}$ (mol $C_3H_8$)(g $Ga/Al_2O_3$)$^{-1}s^{-1}$). $Ga/Al_2O_3$ is moderately selective for propane dehydrogenation, but its dehydrogenation rate is significantly lower than that of $PtZn/SiO_2$. The catalytic performance results confirm that synthesized $PtZn/SiO_2$ catalyst demonstrates high dehydrogenation rate and high olefin selectivity even in the presence of hydrogen, which

indicates that olefins can be produced at higher rate and selectivity than with Ga or MFI zeolite.

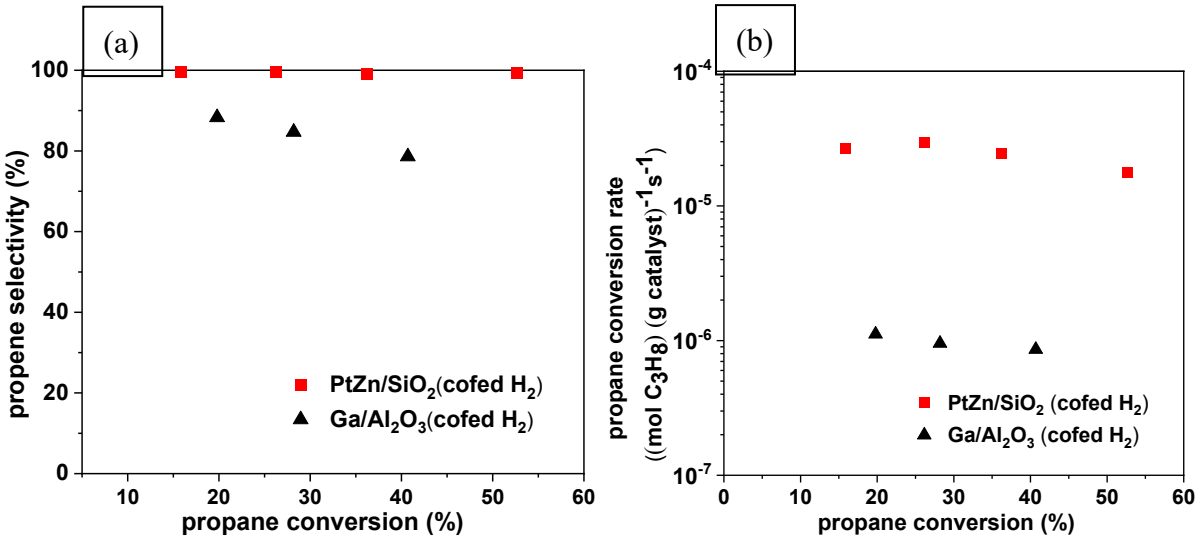


Figure 7. Propane kinetics for $PtZn/SiO_2$ and $Ga/Al_2O_3$ (a) $C_3H_6$ selectivities as a function of $C_3H_8$ conversion (b) the propane conversion rates as a function of $C_3H_8$ conversion. Reaction conditions: cat., 0.01-0.8 g; temperature, 550 °C, pressure, 101 kPa; 2.5% $C_3H_8$, 2.5% $H_2$ balanced with $N_2$; WHSV=7-442 $h^{-1}$

**Product distribution of propane conversion over $PtZn/SiO_2$+ZSM-5 catalysts**

$PtZn/SiO_2$+ZSM-5 bifunctional catalyst composed of $PtZn/SiO_2$ (PA) and ZSM-5 (Z) were studied for propane conversion in this work. The product distribution at different propane conversions was determined for bifunctional catalysts with different weight ratios in gram of ZSM-5 to $PtZn/SiO_2$ (Z/PA) to understand the role of two catalytic functions in the reaction pathways of propane conversion. Figure 8a-8f show product selectivity as a function of propane conversion and Z/PA ratio using 5% propane at 550 °C. The ZSM-5 product distribution was also determined for comparison.

On ZSM-5, the methane selectivity remains at 25-28% in the range of 5-65% propane conversion (Figure 8a). The ethene selectivity is approximately 50% at 5% propane conversion (Figure 8b) and the ratio of ethene selectivity to methane is approximately 2, which is consistent with formation by propane monomolecular cracking. As propane conversion increases, the ethene selectivity decreases, indicating ethene undergoes secondary reactions. The propene

selectivity is 20% at low conversion and decreases as propane conversion increases (Figure 8c). Propene selectivity decreases faster than ethene, suggesting propene is more reactive than ethene on ZSM-5.[6] The non-zero selectivities to methane, ethene and propene at conversion close to zero are indicative that these are primary products. On the contrary, the butenes selectivity is low and approaches zero at the conversion less than 5%. As propane conversion increases, the butenes selectivity increases and goes through a maximum (Figure 8d). The results indicate that butenes are secondary products generated from ethene and propene through the oligomerization-cracking cycle and are further transformed into aromatics. The aromatics selectivity gradually increases as propane conversion increases (Figure 8e). The product selectivity as a function of propane conversion over ZSM-5 is in agreement with prior studies, suggesting that propane undergoes monomolecular cracking, oligomerization, β-scission and aromatization reactions on acid sites.[10]

PtZn/$SiO_2$+ZSM-5 catalysts with different Z/PA ratio are further investigated to understand how Z/PA ratio contributes to product selectivity. Higher Z/PA ratio indicates that the bifunctional catalyst has a higher weight loading of ZSM-5, while low Z/PA ratio is indicative of increasing amounts of PtZn/$SiO_2$ and higher dehydrogenation rates. With Z/PA=50, the methane selectivity is 20% and the ethene selectivity is 40% at 6% propane conversion (Figure 8a-8b). The ratio of ethene to methane selectivity is close to 2, indicating methane and ethene are mostly formed by propane monomolecular cracking on PtZn/$SiO_2$+ZSM-5. However, the lower methane and ethene selectivity and the higher propene selectivity than those on ZSM-5 (Figure 8c), suggesting propane is partly converted by dehydrogenation on the PtZn/$SiO_2$. As propane conversion increases to 55%, the methane selectivity decreases to 15%. This suggests that the mode of the monomolecular cracking of propane by acid sites may by partially inhibited. The maximum butenes selectivity is 4% and slightly higher than that on the ZSM-5 (Figure 8d). The BTX selectivity is low at 10% propane conversion and increases to

approximately 37% at 67% propane conversion (Figure 8e). The 15% higher BTX selectivity on the PtZn/$SiO_2$+ZSM-5 (Z/PA=50) compared to ZSM-5 at the same conversion suggests that the addition of the PtZn/$SiO_2$ enhances BTX formation.

With a decrease in the Z/PA ratio to 6, the methane selectivity decreases to 4% at propane conversion from 15-80% (Figure 8a). The methane selectivity is significantly lower than 25% on ZSM-5 and 20% on PtZn/$SiO_2$+ZSM-5 (Z/PA=50). The ethene selectivity behaves differently depending on the conversion (Figure 8b). At less 15% propane conversion, decrease in the ethene selectivity may be attributed to less monomolecular cracking due to the lower levels of ZSM-5 in the catalyst. In the range of 15-80% propane conversion, ethene slightly increases from 10% to 15% and is likely formed by secondary cracking reactions of higher molecular weight olefins. Eventually, the ethene selectivity decreases to 8% likely due to acid catalyzed conversion to higher molecular weight hydrocarbons, which is consistent with what has been shown for propene conversion on ZSM-5 (Figure 2b). For the PtZn/$SiO_2$+ZSM-5 catalyst with Z/PA=6, the BTX selectivity increases to 52% at 82% propane conversion (Figure 8e).

Further decreasing Z/PA ratio to 1, the methane selectivity remains nearly constant at less than 1% up to propane conversions of almost 70% (Figure 8a). The ethene selectivity is lower than 5% (Figure 8b). The propene selectivity at low propane conversion (<5%) is 95% (Figure 8c), which is close to the dehydrogenation selectivity (99%) on the PtZn/$SiO_2$. The results indicate that propane is primarily converted into propene on the PtZn/$SiO_2$ catalyst, rather than by monomolecular cracking on ZSM-5. As propane conversion increases to 72%, the propene selectivity decreases from 95% to 42%, which is attributed to secondary reactions on acid sites. The maximum of the butenes selectivity (4%) appears at higher propane conversion (50%), implying that the consumption rate of butenes is lower (Figure 8d). The BTX selectivity as a function of propane conversion is higher on all PtZn/$SiO_2$+ZSM-5 catalysts than ZSM-5

regardless of Z/PA ratio, but it is surprising to find that the BTX selectivity with Z/PA=1 is lower than, for example, Z/PA=6 (Figure 8e). By comparing the BTX selectivity at similar propane conversions (40-47%) on ZSM-5 and PtZn/$SiO_2$+ZSM-5 catalysts, it is shown that the BTX selectivity on the former is 10%; while it is 20% and 35% on the latter with Z/PA ratio equal to 50 and 6, respectively. This suggests that increasing dehydrogenation rates can improve aromatics formation, which is consistent with previous results where the dehydrogenation step is rate limiting step for propane aromatization on ZSM-5.[13] However, the BTX selectivity decreases to 20% on the PtZn/$SiO_2$+ZSM-5 catalyst (Z/PA=1) suggesting that the limiting step of aromatics formation is no longer limited by dehydrogenation but is now limited by oligomerization and cyclization by ZSM-5.

Some general trends of product distribution are observed on the PtZn/$SiO_2$+ZSM-5 catalysts regardless of Z/PA ratio. The methane and ethene selectivities on the bifunctional catalysts are lower than those over ZSM-5, while the propene selectivity is higher (Figure 8a-8c). The butenes selectivity over the bifunctional catalysts undergoes a similar trend as that over ZSM-5, going through a maximum as a function of propane conversion increases (Figure 8d). The BTX selectivity on both ZSM-5 and PtZn/$SiO_2$+ZSM-5 catalysts are low at propane conversion below 15% and increases rapidly as the propane conversion increases. At higher propane conversion (>15%), the BTX aromatics selectivity is higher on the bifunctional catalysts than ZSM-5 (Figure 8e). Significant amounts of ethane are observed at propane conversion higher than 40% on the-ZSM-5 and PtZn/$SiO_2$+ZSM-5 catalysts, but ethane selectivity approaches zero at <5% propane conversion, suggesting ethane is a secondary product. (Figure 8f). The results show that addition of the PtZn/$SiO_2$ helps decrease formation of methane and ethene but increases propene, aromatics, and ethane yields.

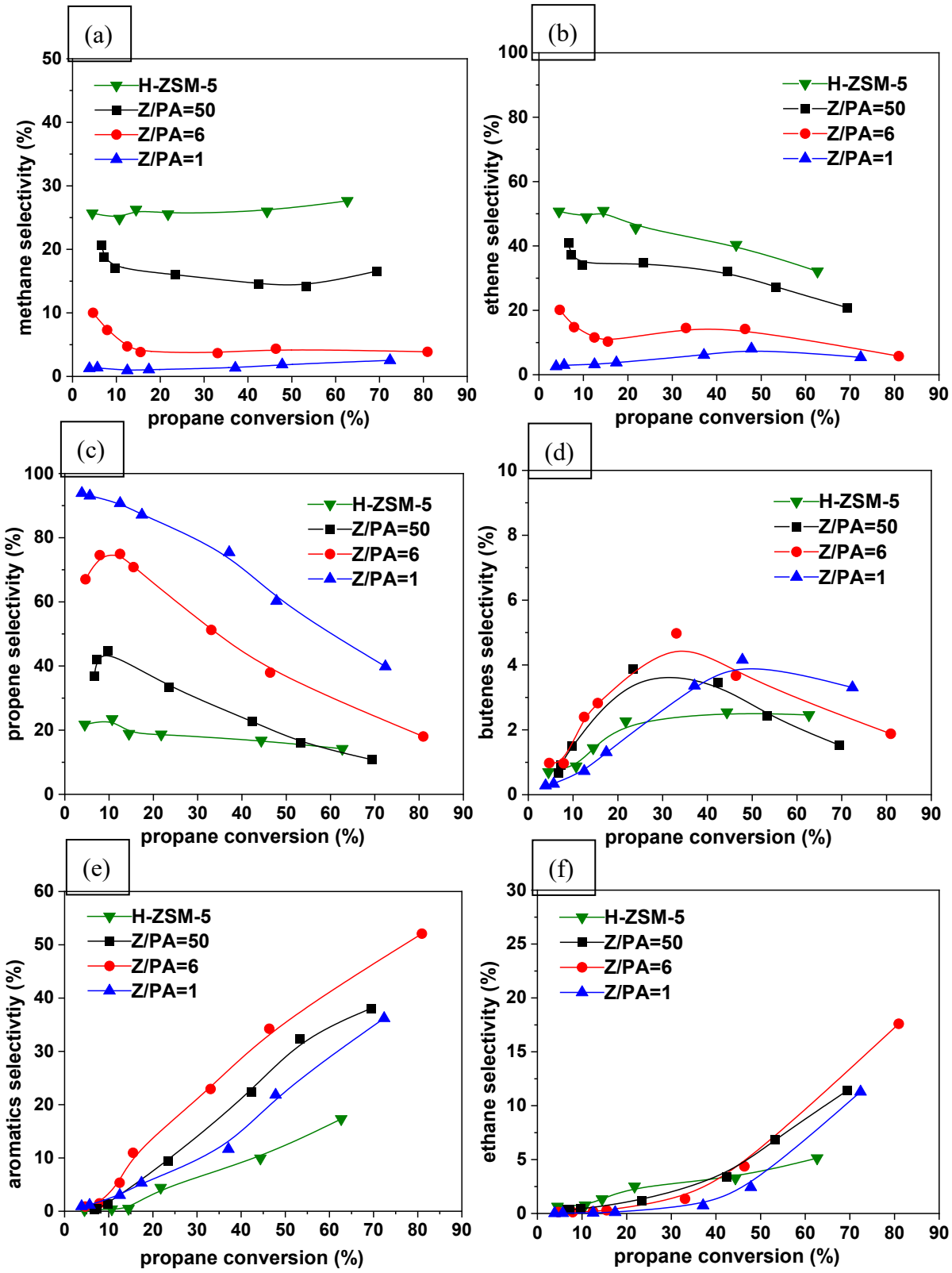


Figure 8. selectivities of (a) methane, (b) ethene, (c) propene, (d) butenes, (e) BTX aromatics (benzene, toluene, xylenes), (f) ethane as a function of propane conversion with a series of Z/PA ratio

Reaction conditions: cat., 0.005-0.7g, temperature, 550°C; pressure, 101 kPa; WHSV, 4-88 $h^{-1}$

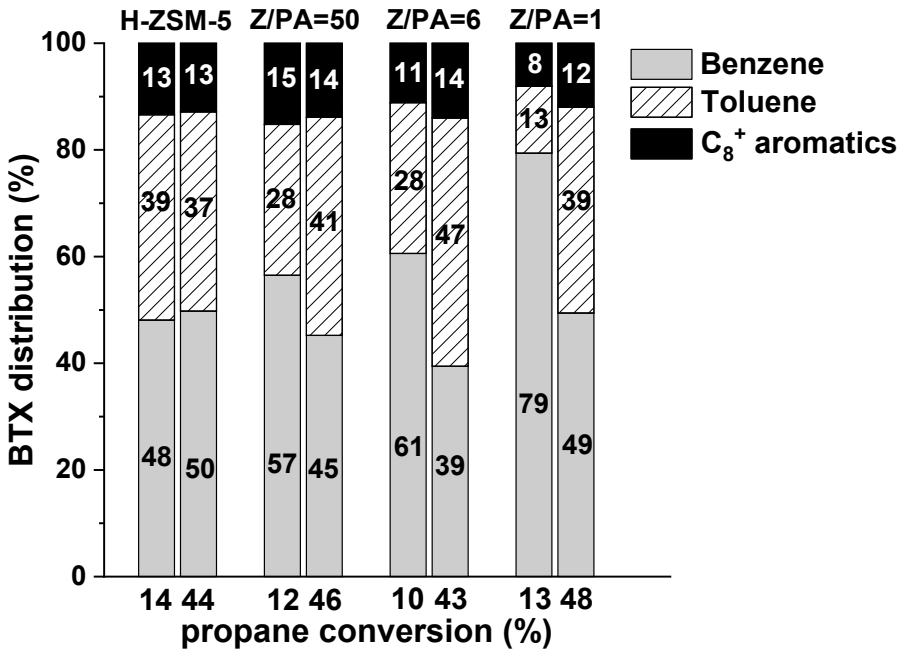


Figure 9. BTX distribution at different propane conversions on ZSM-5 and PtZn/$SiO_2$+ZSM-5 (Z/PA=50, 6, 1) catalysts

The BTX distribution at different propane conversions on ZSM-5 and PtZn/$SiO_2$+ZSM-5 catalysts were also determined in Figure 9. On ZSM-5, the BTX distribution slightly changes with propane conversions and dominant aromatics are benzene (~49%) and toluene (~38%). On the PtZn/$SiO_2$+ZSM-5, benzene percentage is higher compared to ZSM-5 at low propane conversions (10-13%), and benzene percentage increases as Z/PA ratio decreases. For example, with Z/PA=1, aromatics majorly consist of benzene (79%) at 13% propane conversion. These results imply that increasing loading of PtZn catalyst may enhance the dehydrogenation of $C_6$ cyclic hydrocarbons formed by propene dimerization-cyclization and increase the benzene percentage in the BTX distribution at low propane conversions. At medium propane conversions (43-46%), benzene percentage decreases and toluene percentage increases as Z/PA decreases to 6. However, with further decrease in Z/PA ratio to 1, the BTX distribution is similar to that on ZSM-5.

To further understand the correlation between Z/PA ratio and selectivity to methane and BTX, the formation rates of methane and BTX as a function of propane conversion on ZSM-5 and

PtZn/$SiO_2$+ZSM-5 catalysts were determined in Figure 10. The methane formation rates slightly decrease as propane conversion decreases on both catalysts (Figure 10a). As a result, the average methane formation rates at different conversions on ZSM-5 and PtZn/$SiO_2$+ZSM-5 catalysts are used for comparison. On ZSM-5, the average methane formation rate normalized by the amounts of ZSM-5 in the evaluated propane conversion range is about $4.6\times10^{-7}$ (mol $CH_4$)(g ZSM-5)$^{-1}s^{-1}$. On the bifunctional catalysts with Z/PA ratio of 50, 6 and 1, the average methane formation rates normalized by the amounts of ZSM-5 are $2.6\times10^{-7}$, $3.1\times10^{-7}$, $3.5\times10^{-7}$ (mol $CH_4$)(g ZSM-5)$^{-1}s^{-1}$, respectively. Within the scatter of the data, the methane formation rates are independent of Z/PA ratio, suggesting methane is formed primarily by monomolecular cracking and lower methane selectivity in PtZn/$SiO_2$+ZSM-5 is due to the lower loading of ZSM-5. For catalyst with lower Z/PA ratio, the propene selectivity increases (Figure 8c). Therefore, monomolecular cracking and formation of methane is independent of propene concentration. The slight decrease in methane with increasing conversion may, therefore, be due to inhibition of monomolecular cracking by BTX, which increases with increasing propane conversion.

Figure 10b shows BTX formation rate on ZSM-5 and PtZn/$SiO_2$+ZSM-5 catalysts. The BTX formation rate on the former is low ($3.6\times10^{-9}$ (mol BTX)(g catalyst)$^{-1}s^{-1}$) at 10% propane conversion and increases by 200 times ($1.5\times10^{-7}$ (mol BTX)(g catalyst)$^{-1}s^{-1}$) at 50% propane conversion. The Z/PA=50 catalyst has a slightly higher BTX formation rate ($3.8\times10^{-7}$ (mol BTX)(g catalyst)$^{-1}s^{-1}$) at ~50% propane conversion. As the Z/PA ratio decreases to 6, BTX formation rate increases from $3.3\times10^{-8}$ (mol BTX)(g catalyst)$^{-1}s^{-1}$ at 5% propane conversion to $1.5\times10^{-6}$ (mol BTX)(g catalyst)$^{-1}s^{-1}$ at high conversion (~50%), which is 10 times higher than that on ZSM-5. With Z/PA=1, BTX formation rate ($1.5\times10^{-7}$ (mol BTX)(g catalyst)$^{-1}s^{-1}$) is 40 times higher than ZSM-5. At conversion higher than 15%, the rate is nearly the same as that with Z/PA=6.

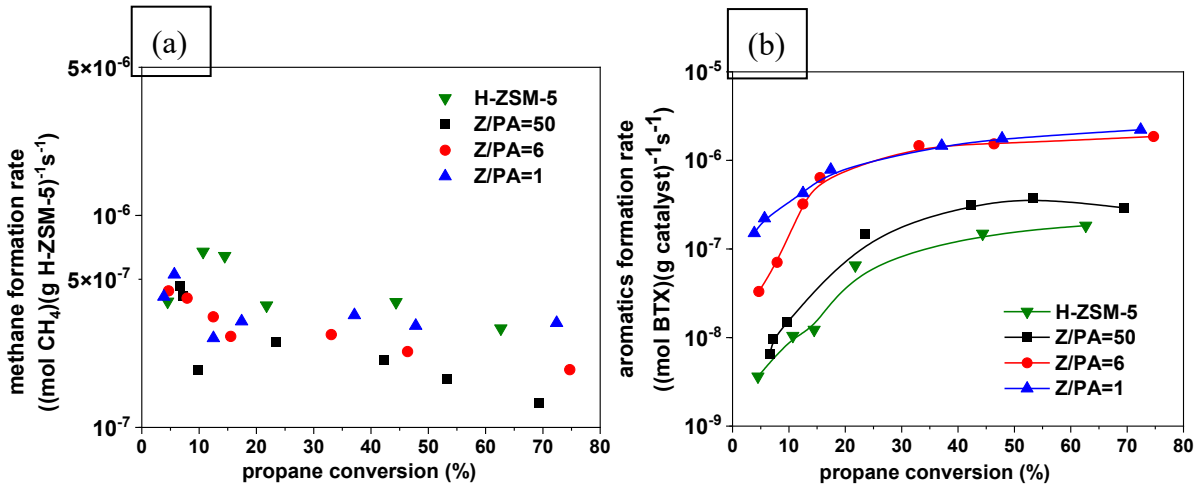


Figure 10. (a) methane formation rate (b) aromatics formation rate as a function of propane conversion on ZSM-5 and PtZn/$SiO_2$+ZSM-5 catalysts

Since the Z/PA=1 catalyst has the lowest methane selectivity (~1%) and highest aromatics formation rate, pure propane (99.99%) at 101 kPa was also evaluated on this catalyst at 550°C. The product distribution is compared to that using 5% propane to understand the influence of propane partial pressure on the product selectivity (Figure 11a-11f). A similar product selectivity as a function of propane conversion is observed at two propane partial pressures. However, higher propane partial pressure has a positive impact on propene conversion since the propene selectivity is lower and decreases much faster than that at lower propane partial pressure at the same conversion (Figure 11c). Meanwhile, the selectivities to butenes and BTX are higher at the higher propane pressure (Figure 11d and 11e). A high BTX selectivity (42%) is observed at 65% propane conversion at higher propane partial pressure, which is 10% higher than that using 5% propane at the same conversion (Figure 11e). Figure 11f shows that ethane selectivity also increases by about 2 times that at lower propane pressure above 30% propane conversion. The increased ethane selectivity occurs at about the same propane conversion as the BTX selectivity increases, suggesting that hydrogen, which formed during aromatics formation, hydrogenates ethene. In summary, these results show that high propane partial

pressure has a beneficial effect on olefin conversion and aromatics formation rate but also leads to higher selectivity to unfavored ethane.

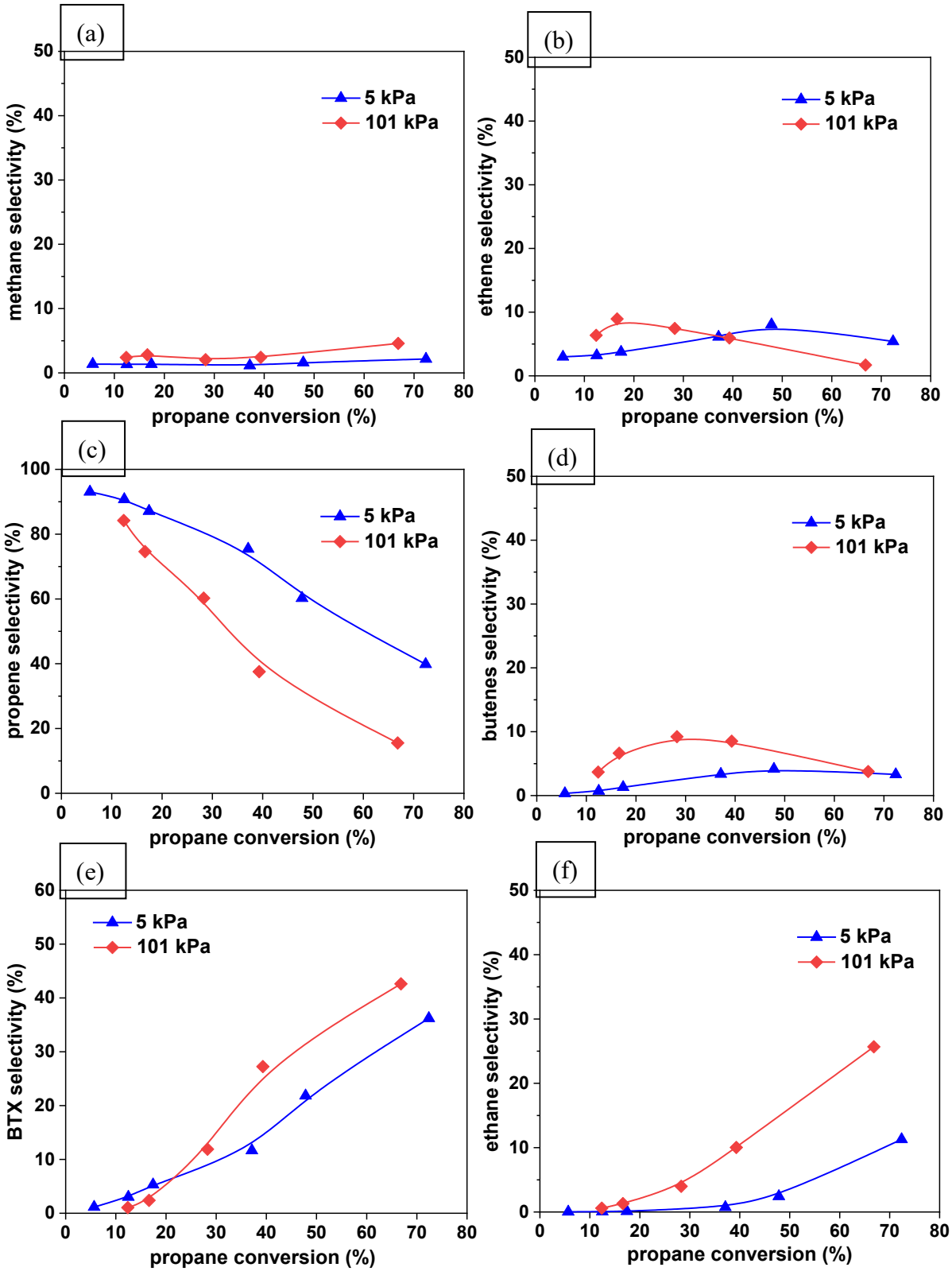


Figure 11. selectivities of (a) methane, (b) ethene, (c) propene, (d) butenes, (e) BTX aromatics, (f) ethane as a

function of propane conversion at 5 kPa and 101 kPa propane partial pressure. Reaction conditions: cat., 0.005-0.1g, temperature, 550℃; total pressure, 101 kPa; Z/PA=1; WHSV=54-1072 $h^{-1}$

**Cyclohexene conversion to aromatics**

Naphthenes or cyclic paraffins and olefins, are likely key intermediates for formation of aromatics. To better understand the aromatization pathway, cyclohexene is selected as a model compound, and the relative rates and selectivity to products over PtZn alloy, $Ga/Al_2O_3$, and ZSM-5 catalysts were determined.

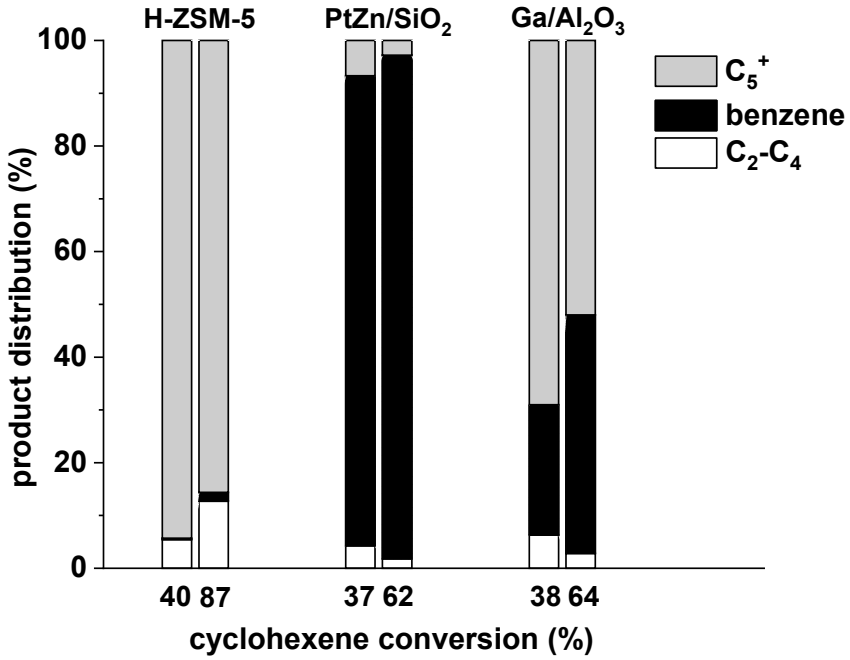


Figure 12. Product distribution of cyclohexene conversion on ZSM-5, $PtZn/SiO_2$ and $Ga/Al_2O_3$ catalysts. Reaction conditions: cat., 0.0015-0.5g, temperature, 550℃; pressure, 101 kPa; cyclohexene partial pressure, 3 kPa[a]; WHSV, 0.3-104 $h^{-1}$

[a] cyclohexene partial pressure is estimated by vapor saturation pressure at 0℃ using Antoine equation

Figure 12 shows that cyclohexene is primarily converted to $C_5^+$ hydrocarbons on ZSM-5 and benzene only formed with low selectivity (2%) at high cyclohexene conversion (87%). Most of $C_5^+$ hydrocarbons are composed of $C_6$ olefins. The detailed product selectivities on each catalyst are listed in Table S2. On the contrary, the $PtZn/SiO_2$ demonstrates higher than 90%

selectivity to benzene with less than 10% selectivity to non-aromatic $C_2$-$C_5^+$ hydrocarbons. In comparison with ZSM-5 and $PtZn/SiO_2$, $Ga/Al_2O_3$ demonstrates a combination of dehydrogenation and cracking selectivity with 25% selectivity to benzene at 38% cyclohexene conversion. The benzene selectivity increases to 45% as the cyclohexene conversion increases to 64%.

Table 4. The apparent rates of cyclohexene conversion and the formation of benzene and $C_2$-$C_5^+$ cracking products over ZSM-5, $PtZn/SiO_2$ and $Ga/Al_2O_3$ catalysts [a]

| Catalysts | Cyclohexene conversion rate (mol $C_6H_{10}$)(g catalyst)$^{-1}$s$^{-1}$ | Benzene formation rate (mol benzene)(g catalyst)$^{-1}$s$^{-1}$ | Cracking rate (mol $C_2$-$C_5^+$)(g catalyst)$^{-1}$s$^{-1}$ |
|---|---|---|---|
| ZSM-5 | $5.4\times10^{-4}$ | $1.3\times10^{-6}$ | $5.3\times10^{-4}$ |
| $PtZn/SiO_2$ | $3.1\times10^{-4}$ | $2.8\times10^{-4}$ | $3.5\times10^{-5}$ |
| $Ga/Al_2O_3$ | $3.8\times10^{-6}$ | $9.5\times10^{-7}$ | $2.9\times10^{-8}$ |

[a] The rates are estimated at 38-40% cyclohexene conversion.

The cyclohexene conversion rates over each catalyst were further estimated (Table 4). The cyclohexene conversion rates on ZSM-5 and $PtZn/SiO_2$ are similar, $5.4\times10^{-4}$ (mol $C_6H_{10}$)(g ZSM-5)$^{-1}$s$^{-1}$ and $3.1\times10^{-4}$ (mol $C_6H_{10}$)(g $PtZn/SiO_2$)$^{-1}$s$^{-1}$ respectively; while $Ga/Al_2O_3$ is $3.8\times10^{-6}$ (mol $C_6H_{10}$)(g $Ga/Al_2O_3$)$^{-1}$s$^{-1}$, approximately 100 times lower. Benzene formation and cracking rates are estimated by multiplying the cyclohexene conversion rate with the carbon selectivity to benzene and $C_2$-$C_5^+$ hydrocarbons, respectively. $C_2$-$C_5^+$ hydrocarbons are indicative of non-aromatic products. The benzene formation rates on ZSM-5 and $Ga/Al_2O_3$ were similar, $1.3\times10^{-6}$ (mol benzene)(g ZSM-5)$^{-1}$s$^{-1}$ and $9.5\times10^{-7}$ (mol benzene)(g $Ga/Al_2O_3$)$^{-1}$s$^{-1}$, respectively. Even though $Ga/Al_2O_3$ has higher selectivity to benzene, the conversion rate is lower than ZSM-5 and, therefore, the benzene formation rate is comparable on the ZSM-5 and $Ga/Al_2O_3$. On the contrary, the benzene formation rate on $PtZn/SiO_2$ is $2.8\times10^{-4}$ (mol benzene)(g $PtZn/SiO_2$)$^{-1}$s$^{-1}$, which is 200 times higher than that on ZSM-5. However, cracking rate on ZSM-5 ($5.3\times10^{-4}$ (mol $C_2$-$C_5^+$)(g ZSM-5)$^{-1}$s$^{-1}$) is the same order of

magnitude of the benzene formation rate on the $PtZn/SiO_2$.

**The strategy to minimize methane formation**

The propane conversion rate on ZSM-5 is 1.5 times higher than that on the $Ga/Al_2O_3$ (Table 2). Based on the difference in rates, 60% of propane will react with ZSM-5 by propane monomolecular cracking and the remaining 40% will react with $Ga/Al_2O_3$ by dehydrogenation. Based on the selectivities for each catalyst, the primary product mixture on ZSM-5 will consist of ~17% methane and ~43% light olefins with some higher molecular weight hydrocarbons, while the product for $Ga/Al_2O_3$ will consist of 39% selectivity to propene and less than 1% methane.

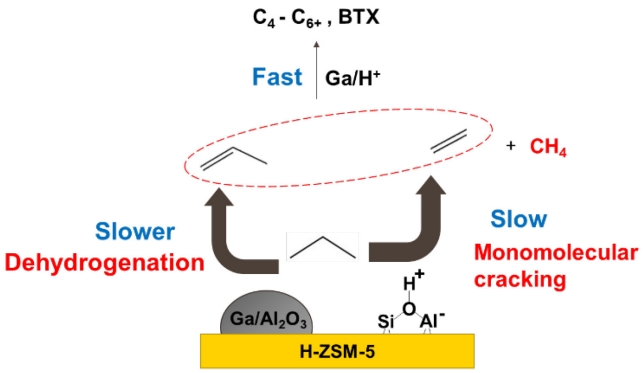


Figure 13. relative kinetics of light gas formation pathways on the $Ga/Al_2O_3$+ZSM-5 catalysts

While Ga has higher propene selectivity, Ga dehydrogenation rates and ZSM-5 monomolecular cracking rates are in the same order of magnitude. As a result, significant amounts of propane will react with the ZSM-5 to form light olefin and unreactive methane simultaneously. By comparing the conversion rates of alkanes and olefins on ZSM-5, olefins are significantly more reactive than alkanes (Figure 2b), and since olefins can be eventually converted to higher molecular weight hydrocarbons with little methane or ethane, these results suggest that the majority of light gas is caused by monomolecular cracking on ZSM-5 on this bifunctional

catalyst. The relative kinetics of the steps for dehydroaromatization of propane on the $Ga/Al_2O_3$+ZSM-5 catalyst is summarized qualitatively in Figure 13.

Accordingly, we hypothesize that methane formation can be minimized by significantly enhancing propane conversion rate by dehydrogenation and reducing the propane conversion rate on ZSM-5. The strategy is to balance the alkane and olefin conversion rates on two catalytic functions to ensure that propane will be primarily activated by dehydrogenation catalyst. Since olefin reactivity is much higher than alkane, olefin conversion rate on ZSM-5 is still high even with decreasing amounts of zeolite. Based on this strategy, the bifunctional catalyst requires a highly active dehydrogenation catalyst with much higher propane conversion rate than ZSM-5. The previous study with Pt/ZSM-5 reported that propene is the only primary product from propane conversion, which suggests propane conversion occurs on Pt sites. However, monometallic Pt has two drawbacks, low dehydrogenation selectivity and fast deactivation. For example, a 20wt% selectivity to methane on the Pt/ZSM-5 was still observed. For Pt/ZSM-5, methane and part of ethane results from hydrogenolysis of propane on Pt sites.[24] In addition, metallic Pt sites deactivates rapidly due to fast coke formation. As a result, very quickly, Pt/ZSM-5 catalysts are very similar to ZSM-5. The $PtZn/SiO_2$ catalyst (PtZn alloy) has much higher dehydrogenation rates, olefin selectivity and stability than monometallic Pt. However, the methane selectivity is still high at 15-20% on the $PtZn/SiO_2$+ZSM-5 (Z/PA=50), i.e., a catalyst with high loading of ZSM-5. As Z/PA ratio decreases, the methane selectivity decreases and BTX selectivity increases. This indicates that the optimal selectivity is dependent on balancing the alkane dehydrogenation and olefin conversion rates, while limiting monomolecular cracking. Accordingly, the product distribution can be controlled by adjusting the loading of each component ($PtZn/SiO_2$ and ZSM-5) in the bifunctional catalyst. Because olefins are much more reactive than alkanes on ZSM-5, the rate of monomolecular cracking can be minimized, while maintaining high olefin conversions with

lower loadings of ZSM-5. Figure 8a-8c show that the methane and ethene selectivities decrease and propene selectivity increases at low propane conversion (<5%) when Z/PA ratio decreases from 50 to 1, which is consistent with our hypothesis. As the loading of the $PtZn/SiO_2$ increases (lower Z/PA ratio), propane conversion rate on the $PtZn/SiO_2$ becomes significantly higher relatively to that on ZSM-5. Low methane selectivity (<2%) and high propene selectivity (95%) at 5% propane conversion on the Z/PA=1 catalyst suggests that $PtZn/SiO_2$ propane dehydrogenation dominates over ZSM-5 monomolecular cracking. At high conversions, the decreasing propene selectivity indicates that propene is sufficiently reactive despite the lower levels of ZSM-5 in the catalyst.

Based on the results in Figure 10, methane formation rates normalized by the amount of ZSM-5 in the bifunctional catalyst regardless of Z/PA ratio are similar with those on ZSM-5, which suggests that monomolecular cracking is still occurring in all catalysts. Consequently, the possibility that decreasing methane selectivity on the $PtZn/SiO_2$+ZSM-5 catalysts is due to suppressed monomolecular cracking by higher olefin concentration can be excluded. The low methane selectivity is resulting from increasing propane conversion rate on the selective dehydrogenation catalyst and decreasing the propane monomolecular cracking on ZSM-5 while maintaining high olefin conversion rates.

**Propane conversion pathway comparison**

Figure 14 compares the dominant reaction pathways for ZSM-5, $Ga/Al_2O_3$+ZSM-5 and $PtZn/SiO_2$+ZSM-5 catalysts. The blue and orange colored-arrows are used to indicate the dominant reaction pathways catalyzed by acid and metal catalysts, respectively, while the width of the colored-arrows exhibit the relative rate of individual reactions qualitatively. Figure 14a shows the typical propane conversion pathway catalyzed by ZSM-5. Propane is converted to methane, ethene and propene by monomolecular cracking. Ethene and propene rapidly undergo

oligomerization, cracking and cyclization to produce $C_3$-$C_6$ as well as cyclic hydrocarbons. The cyclohexene cracking rate is significantly higher than benzene formation rate, suggesting most of cyclic hydrocarbons will return to the oligomerization-cracking cycle to produce olefins and only few are converted into aromatics by hydrogen transfer. Thus, aromatics formation by ZSM-5 is kinetically slow.

With addition of Ga, Ga/ZSM-5 bifunctional catalysts have higher propane conversion rates and higher aromatics selectivity.[25–31] The Ga/$Al_2O_3$+ZSM-5 catalyst is used as a representative bifunctional catalyst to demonstrate propane conversion reaction pathway (Figure 14b). Based on conversion rates on ZSM-5 and Ga/$Al_2O_3$ (Table 2), propane is converted at similar rates by ZSM-5 monomolecular cracking and Ga dehydrogenation. Although the methane selectivity of Ga/ZSM-5 is improved relative to ZSM-5, there is still a significant selectivity from monomolecular cracking in this bifunctional catalyst. The light olefins in the reaction mixture go through a similar reaction pathway to those on ZSM-5 to form higher molecular weight olefins, including cyclic olefins. As indicated in the Table 4, the cyclohexene conversion rate on ZSM-5 is significantly higher than on Ga/$Al_2O_3$, suggesting that cyclic olefins primarily crack on the former rather than dehydrogenate to aromatics on the latter. The benzene formation rates on ZSM-5 and Ga/$Al_2O_3$ are similar, suggesting the major role of Ga/$Al_2O_3$ is to form some propene and to facilitate the dehydrogenation step of cyclic olefins to aromatics. This is indicative of higher rate and selectivity to aromatics on the bifunctional Ga/ZSM-5 catalysts.

The PtZn/$SiO_2$+ZSM-5 catalyst not only has a low methane selectivity, but also has a higher rate and selectivity to BTX than ZSM-5 and Ga/ZSM-5. Figure 14c summarizes the effect of the PtZn/$SiO_2$ on the dominant propane conversion pathways over the PtZn/$SiO_2$+ZSM-5 bifunctional catalyst. The dash arrow is utilized to highlight the reaction pathways that have been minimized. PtZn/$SiO_2$ has a higher propene selectivity; thus, there is little methane formed by hydrogenolysis. In addition, the high dehydrogenation rate has two beneficial effects. First,

it increases propene selectivity and allows for a lower loading of ZSM-5, resulting in a much smaller contribution of methane from monomolecular cracking by ZSM-5. Second, it has a much higher selectivity and rate of aromatics formation than ZSM-5 or Ga; thus, the BTX formation rates are higher, suggesting that cyclohexene is primarily converted to benzene by the dehydrogenation pathway.

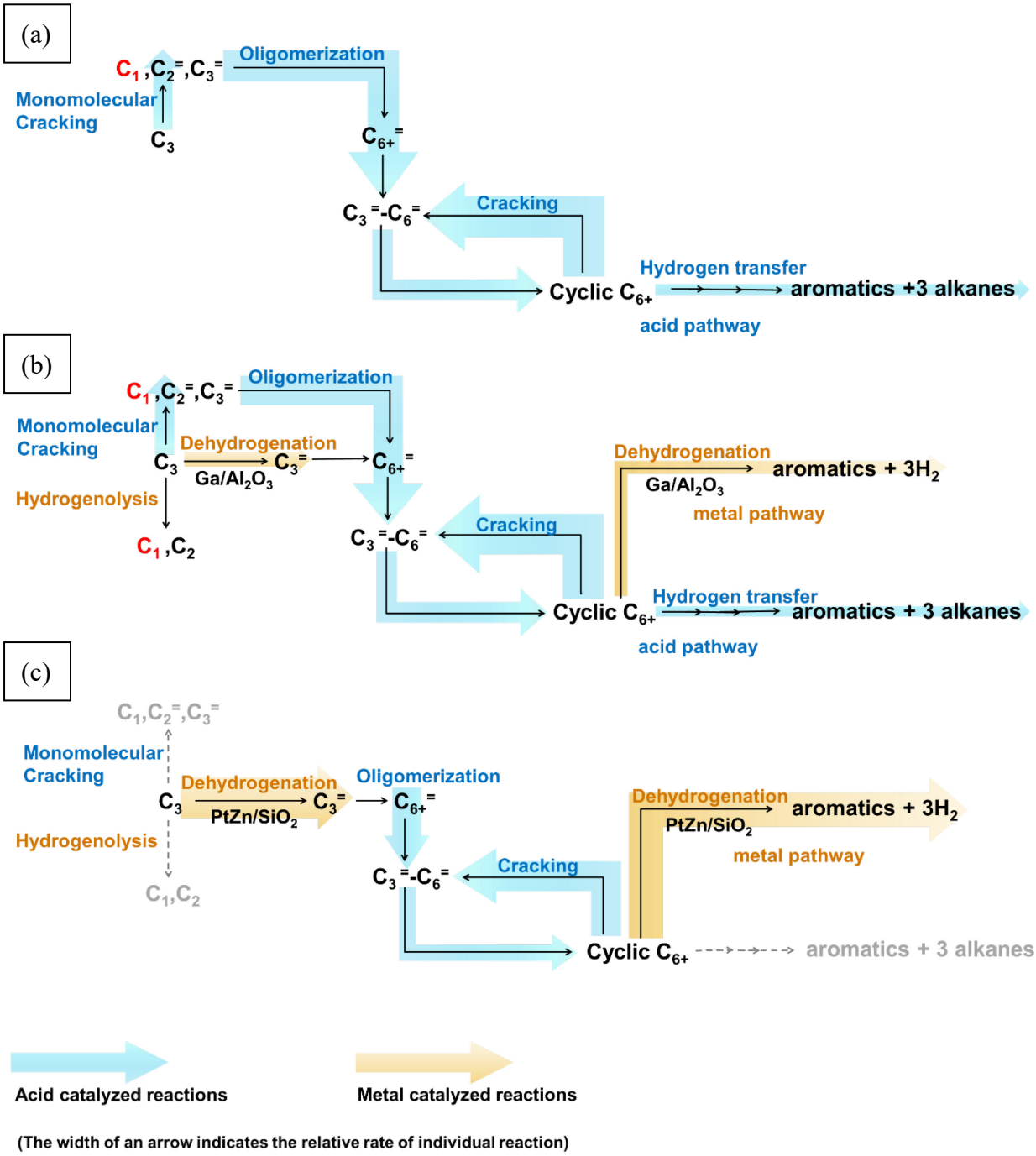


Figure 14. (a) Dominant reaction pathways on (a) ZSM-5 (b) $Ga/Al_2O_3$+ZSM-5 (c) $PtZn/SiO_2$+ZSM-5 catalysts

As Z/PA ratio decreases from 50 to 6, the aromatics selectivity increases at the constant propane conversion. This suggests the dehydrogenation reaction is the rate limiting step for aromatics formation since the aromatics are formed at a higher rate with increasing amounts of $PtZn/SiO_2$ in the bifunctional catalyst. With Z/PA=6, a maximum selectivity of 52% to BTX at about 80% propane conversion is produced without making significant amount of methane (<5%). The BTX selectivity is estimated to exceed 85% at full recycle of all reactive intermediates with byproducts of 5% methane and 10% ethane. However, as Z/PA ratio further decreases from 6 to 1, the BTX selectivity decreases. This indicates that increasing dehydrogenation rate no longer enhances the aromatics formation rate and suggests that aromatics formation is likely limited by acid catalyzed reactions, i.e., oligomerization and cyclization.

The results of product selectivity using higher propane partial pressure suggest the reaction pathway is similar to that using dilute propane. The selectivity of methane and ethene increases slightly, indicating monomolecular cracking is slightly affected by the propane partial pressure (Figure 11a and 11b). The decrease in propene selectivity as a function of propane conversion implies that the olefin oligomerization rate is higher at higher propane pressure (Figure 11c). This result agrees with higher selectivity to butenes and aromatics using higher propane partial pressure (Figure 11d and 11e). Nevertheless, aromatics formation involves oligomerization steps on acid sites and dehydrogenation steps on PtZn sites, which favor high and low pressures, respectively.[7]

At higher propane pressure, the ethane selectivity is higher than at lower partial pressure (Figure 11f). Since the methane selectivity is low, it is less likely that ethane is formed by either propane hydrogenolysis on $PtZn/SiO_2$, or monomolecular cracking followed by ethene hydrogenation. Since the ethane selectivity changes in a similar way as the aromatics selectivity,

ethane is inferred to be a secondary product formed along with aromatics and co-produced hydrogen, for example, by aromatics dealkylation along with ethene hydrogenation.[8,50–52] Generally, activation of light alkane to olefin is thought as the rate limiting step for propane dehydroaromatization.[1,53] As a result, high activity zeolites are utilized in the bifunctional catalysts to enhance not only propane activation but the rate and selectivity to aromatics by rapidly converting generated olefins to aromatics. However, significant monomolecular cracking occurs on catalysts with high loading of ZSM-5, and eventually formation of methane limits the production of aromatics. The selectivity to methane can be reduced by adjusting the Z/PA ratio in the PtZn/$SiO_2$+ZSM-5 to balance the rates of alkane and olefin conversion. With high loading of PtZn/$SiO_2$, the propane conversion gives primarily propene, leading to higher selectivity of higher molecular weight hydrocarbons, including $C_4^+$ paraffins, olefins and BTX. By balancing the dehydrogenation rate with PtZn alloy and the olefin conversion rates by ZSM-5, higher yields of valuable products can be obtained.

**Conclusions**

Comparison of the relative rate and selectivity of propane conversion on Ga/$Al_2O_3$ and ZSM-5, methane is suggested to form predominantly by monomolecular cracking on ZSM-5. While Ga increases the propene selectivity and rate through propane dehydrogenation, there is still a significant contribution by monomolecular cracking with high methane selectivity from ZSM-5 in the bifunctional catalyst.

By utilizing the PtZn/$SiO_2$ (PtZn alloy) with very high dehydrogenation rate and selectivity, significant improvements in the product distribution are observed. Firstly, the methane selectivity decreases to less than 5% because the hydrogenolysis and monomolecular cracking pathways are minimized. Since the rate and selectivity of cyclohexene to benzene on PtZn/$SiO_2$ is significantly higher than that on Ga/$Al_2O_3$ and ZSM-5, aromatics are formed at a higher rate

by the metal pathway (dehydrogenation) over the former catalysts instead of acid pathway (hydrogen transfer) over the latter two. To achieve the optimal product selectivity, it is necessary to balance the propane dehydrogenation and olefin conversion rates by changing the ratio of PtZn alloy and ZSM-5. This work also highlights the difference in the reaction pathways for propane dehydroaromatization for ZSM-5, Ga/ZSM-5 and PtZn/$SiO_2$+ZSM-5 catalysts.

**Associated Content**

The Supporting Information is available free of charge online.

Catalyst stability and detailed product selectivity.

**Acknowledgement**

This work was supported by the NSF/ERC CISTAR, which is supported by the National Science Foundation under Cooperative Agreement No. EEC-164772. Acquisition of the TEM was supported by the NSF MRI grant DMR-1828731.

## References


(1) National Academies of Sciences. Engineering and Medicine. *The Changing Landscape of Hydrocarbon Feedstocks for Chemical Production: Implications for Catalysis: Proceedings of a Workshop*; 2016. https://doi.org/10.17226/23555.

(2) Csicsery, S. M. Dehydrocyclodimerization I. Dehydrocyclodimerization of Butanes over Supported Platinum Catalyst. *J. Catal.* **1970**, *17*, 207–215.

(3) Csicsery, S. M. Dehydrocyclodimerization. *Ind. Eng. Chem. Process Des. Dev.* **1979**, *18* (2), 191–197. https://doi.org/10.1021/i260070a001.

(4) Csicsery, S. M. Dehydrocyclodimerization II . Dehydrocyclodimerization over Supported of Propane and Pentane over Supported Platinum Catalyst. *J. Catal.* **1970**, *17*, 216–218.

(5) Csicsery, S. M. Dehydrocyclodimerization V. The Mechanism of the Reaction. *J. Catal.* **1970**, *18*, 30–32.

(6) Lukyanov, D. B.; Gnep, N. S.; Guisnet, M. R. Kinetic Modeling of Ethene and Propene Aromatization HZSM-5. *Ind. Eng. Chem. Res* **1994**, *33*, 223–234. https://doi.org/10.1021/ie00026a008.

(7) Quann, R. J.; Green, L. A.; Tabak, S. A.; Krambeck, F. J. Chemistry of Olefin Oligomerization ZSM-5 Catalyst. *Ind. Eng. Chem. Res.* **1988**, *27*, 565–570. https://doi.org/10.1021/ie00076a006.

(8) Ono, Y. Transformation of Lower Alkanes into Aromatic Transformation of Lower Alkanes into Aromatic Hydrocarbons over ZSM-5 Zeolites. *Catal. Rev.* **1992**, No. 34(3), 179–226. https://doi.org/10.1080/01614949208020306.

(9) Giannetto, G.; Monque, R.; Galiasso, R.; Galiass, R. Transformation of LPG into Aromatic Hydrocarbons and Hydrogen over Zeolite Catalysts. *Catal. Rev. Eng.* **1994**, *36(2)*, 271–304. https://doi.org/10.1080/01614949408013926.

(10) Kitagawa, H.; Sendoda, Y.; Ono, Y. Transformation of Propane into Aromatic over ZSM-5 Zeolites. *J. Catal.* **1986**, *101*, 12–18.

(11) Guisnet, M.; Gnep, N. S. Mechanism of Short-Chain Alkane Transformation over Protonic Zeolites .

Alkylation , Disproportionation and Aromatization. *Appl. Catal. A Gen.* **1996**, *146*, 33–64.

(12) Caeiro, G.; Carvalho, R. H.; Wang, X.; Lemos, M. A. N. D. A.; Lemos, F.; Guisnet, M.; Ramˆ, F. Activation of C2–C4 Alkanes over Acid and Bifunctional Zeolite Catalysts. *J. Mol. Catal. A Chem.* **2006**, *255*, 131–158. https://doi.org/10.1016/j.molcata.2006.03.068.

(13) Guisnet, M.; Gnep, N. S.; Aittaleb, D.; Doyemet, Y. J. Conversion of Light Alkanes into Aromatic Hydrocarbons VI. Aromatization of C2-C4 Alkanes on H-ZSM-5 - Reaction Mechanisms. *Appl. Catal. A, Gen.* **1992**, No. 87, 255–270.

(14) Haag, W. O.; Dessau, R. M. Proceedings, 8th International Congress on Catalysis, Berlin, 1984,; 1984; Vol. Vol 2, p Dechema, Frankfurt-am-Main, 305.

(15) Bhan, A.; Delgass, W. N. Propane Aromatization over HZSM-5 and Ga/HZSM-5 Catalysts. *Catal. Rev.* **2008**, No. 50:1, 19–151. https://doi.org/10.1080/01614940701804745.

(16) Krannila, H.; Haag, W. O.; Gates, B. C. Monomolecular and Bimolecular Mechanisms of Paraffin Cracking : N-Butane Cracking Catalyzed by HZSM-5. *J. Catal.* **1992**, No. 135, 115–124.

(17) Mole, T.; Anderson, J. R.; Creer, G. The Reaction of Propane over ZSM-5-H and ZSM-5-Zn Zeolite Catalyst. *Appl. Catal.* **1985**, *17*, 141–154.

(18) Sirokman, G.; Sendoda, Y.; Ono, Y. Conversion of Pentane into Aromatics over ZSM-5 Zeolites. *ZEOLITES* **1986**, *6*, 299–303.

(19) Haag, W. O. Catalytic Conversion of Propane to Aromatics, Effects of Adding Ga and or Pt to HZSM-5. *J. Catal.* **1994**, No. 149, 465–473.

(20) Guisnet, M.; Gnep, N. S. Aromatization of Short Chain Alkanes on Zeolite Catalysts. **1992**, *89*, 1–30.

(21) Biscardi, J. A.; Iglesia, E. Reaction Pathways and Rate-Determining Steps in Reactions of Alkanes on H-ZSM5 and Zn/H-ZSM5 Catalysts. *J. Catal.* **1999**, *182*, 117–128.

(22) Price, G. L.; Kanazirev, V.; Dooley, K. M.; Hart, V. I. On the Mechanism of Propane Dehydrocyclization over Cation-Containing, Proton-Poor MFI Zeolite. *J. Catal.* **1998**, *173*, 17–27.

(23) Noh, G.; Shi, Z.; Zones, S. I.; Iglesia, E. Isomerization and β-Scission Reactions of Alkanes on

Bifunctional Metal- Acid Catalysts : Consequences of Confinement and Diffusional Constraints on Reactivity and Selectivity. *J. Catal.* **2018**, *368*, 389–410. https://doi.org/10.1016/j.jcat.2018.03.033.

(24) Gnep, N. S.; Doyemet, J. Y.; Ribeiro, F. R.; Guisnet, M. Conversion of Light Alkanes into Aromatic Hydrocarbons : 1-Dehydrocyclodimerization Propane on PtHZSM-5 Catalysts. *Appl. Catal.* **1987**, *35*, 93–108.

(25) Price, G. L.; Kanazirev, V. Ga2O3/HZSM-5 Propane Aromatization Catalysts : Formation of Active Centers via Solid-State Reaction. *J. Catal.* **1990**, *126*, 267–278.

(26) Jacobs, P. A.; Chemistry, Z.; Henares, F. De. DEHYDROCYCLODIMERIZATION OF SHORT CHAIN ALKANES ON Ga/ZSM-5 AND Ga/BETA ZEOLITES. *Zeolite Chem. Catal.* **1991**, No. 5, 409–416.

(27) Dooley, K. M.; Chang, C.; Price, G. L. Effects of Pretreatments on State of Gallium and Aromatization Activity of Gallium/ZSM-5 Catalysts. *Appl. Catal. A Gen.* **1992**, *84*, 17–30.

(28) Biscardi, A.; Iglesia, E. Structure and Function of Metal Cations in Light Alkane Reactions. *Catal. Today* **1996**, *31*, 207–231.

(29) Choudhary, V. R.; Kinage, A. K.; Choudhary, T. V. Simultaneous Aromatization of Propane and Higher Alkanes or Alkenes over H-GaAlMFI Zeolite. *Chem. Commun.* **1996**, 2545–2546.

(30) Yashima, T.; Fujita, S.; Komatsu, T. Reaction Scheme of Aromatization of Butane over Ga Loaded HZSM-5 Catalyst. □ □ □ □ □ *Sekiyu Gakkaishi* **1998**, *41* (1), 37–44.

(31) Ishaq, M.; Khan, M. A.; Yashima, T. Mechanism of Butane Transformation. *J. Chinese Chem. Soc.* **2000**, *47*, 1137–1143.

(32) Al-Zahrani, S. M. Catalytic Conversion of LPG to High-Value Aromatics : The Current State of the Art and Future Predictions. *Dev. Chem. Eng. Miner. Process* **1998**, *6*, 101–120.

(33) Rodrigues, V. D. O.; Júnior, A. C. F. On Catalyst Activation and Reaction Mechanisms in Propane Aromatization on Ga / HZSM5 Catalysts. *Appl. Catal. A, Gen.* **2012**, *435–436*, 68–77. https://doi.org/10.1016/j.apcata.2012.05.036.

(34) Gnep, N. S.; Doyemet, J. Y.; Seco, A. M.; Ribeiro, F. R.; Guisnet, M. Conversion of Light Alkanes to

Aromatic Hydrocarbons II. Role of Gallium Species in Propane Transformation on GaHZSM5 Catalysts. *Appl. Catal.* **1988**, *43*, 155–166.

(35) Jentoft, F. C.; Gates, B. C. Solid-Acid-Catalyzed Alkane Cracking Mechanisms : Evidence from Reactions of Small Probe Molecules. **1997**, *4*, 1–13.

(36) Choudhary, V. R.; Panjala, D.; Banerjee, S. Aromatization of Propene and n -Butene over H-Galloaluminosilicate ( ZSM-5 Type ) Zeolite. **2002**, *231*, 243–251.

(37) de Jong, K. P. *Synthesis of Solid Catalysts*; Wiley-VCH Verlag GmbH & Co. KGaA: Weinheim, 2009.

(38) Miller, J. T.; Schreier, M.; Kropf, A. J.; Regalbuto, J. R. A Fundamental Study of Platinum Tetraammine Impregnation of Silica: 2. The Effect of Method of Preparation, Loading, and Calcination Temperature on (Reduced) Particle Size. *J. Catal.* **2004**, *225* (1), 203–212. https://doi.org/10.1016/j.jcat.2004.04.007.

(39) Ressler, T. WinXAS: A Program for X-Ray Absorption Spectroscopy Data Analysis under MS-Windows. *J. Synchrotron Radiat.* **1998**, *5* (2), 118–122. https://doi.org/10.1107/S0909049597019298.

(40) Cybulskis, V. J.; Bukowski, B. C.; Tseng, H. T.; Gallagher, J. R.; Wu, Z.; Wegener, E.; Kropf, A. J.; Ravel, B.; Ribeiro, F. H.; Greeley, J.; Miller, J. T. Zinc Promotion of Platinum for Catalytic Light Alkane Dehydrogenation: Insights into Geometric and Electronic Effects. *ACS Catal.* **2017**, *7* (6), 4173–4181. https://doi.org/10.1021/acscatal.6b03603.

(41) Cybulskis, V. J.; Pradhan, S. U.; Lovón-Quintana, J. J.; Hock, A. S.; Hu, B.; Zhang, G.; Delgass, W. N.; Ribeiro, F. H.; Miller, J. T. The Nature of the Isolated Gallium Active Center for Propane Dehydrogenation on Ga/SiO2. *Catal. Letters* **2017**, *147* (5), 1252–1262. https://doi.org/10.1007/s10562-017-2028-2.

(42) LiBretto, N. J.; Xu, Y.; Quigley, A.; Edwards, E.; Nargund, R.; Vega-Vila, J. C.; Caulkins, R.; Saxena, A.; Gounder, R.; Greeley, J.; Zhang, G.; Miller, J. T. Olefin Oligomerization by Main Group Ga3+ and Zn2+ Single Site Catalysts on SiO2. *Nat. Commun.* **2021**, *12* (1), 1–9. https://doi.org/10.1038/s41467-021-22512-6.

(43) Szeto, K. C.; Jones, Z. R.; Merle, N.; Rios, C.; Gallo, A.; Le Quemener, F.; Delevoye, L.; Gauvin, R.

M.; Scott, S. L.; Taoufik, M. A Strong Support Effect in Selective Propane Dehydrogenation Catalyzed by Ga(i-Bu)3 Grafted onto γ-Alumina and Silica. *ACS Catal.* **2018**, *8* (8), 7566–7577. https://doi.org/10.1021/acscatal.8b00936.

(44) Sattler, J. J. H. B.; Ruiz-Martinez, J.; Santillan-Jimenez, E.; Weckhuysen, B. M. Catalytic Dehydrogenation of Light Alkanes on Metals and Metal Oxides. *Chem. Rev.* **2014**, *114* (20), 10613–10653. https://doi.org/10.1021/cr5002436.

(45) Den Hollander, M. A.; Wissink, M.; Makkee, M.; Moulijn, J. A. Gasoline Conversion: Reactivity towards Cracking with Equilibrated FCC and ZSM-5 Catalysts. *Appl. Catal. A Gen.* **2002**, *223* (1–2), 85–102. https://doi.org/10.1016/S0926-860X(01)00745-1.

(46) Zhu, X.; Liu, S.; Song, Y.; Xu, L. Catalytic Cracking of C4 Alkenes to Propene and Ethene: Influences of Zeolites Pore Structures and Si/Al2 Ratios. *Appl. Catal. A Gen.* **2005**, *288* (1–2), 134–142. https://doi.org/10.1016/j.apcata.2005.04.050.

(47) Jun, J. W.; Kim, T. W.; Il Hong, S.; Kim, J. W.; Jhung, S. H.; Kim, C. U. Selective and Stable Production of Ethylene from Propylene over Surface-Modified ZSM-5 Zeolites. *Catal. Today* **2018**, *303* (May 2017), 86–92. https://doi.org/10.1016/j.cattod.2017.10.004.

(48) Shibata, M.; Kitagawa, H.; Sendoda, Y.; Ono, Y. Transformation of Propene into Aromatic Hydrocarbons over ZSM-5 Zeolites. *Stud. Surf. Sci. Catal.* **1986**, *28*, 717–724. https://doi.org/10.1016/S0167-2991(09)60939-3.

(49) Lei, Y.; Jelic, J.; Nitsche, L. C.; Meyer, R.; Miller, J. Effect of Particle Size and Adsorbates on the L3, L2 and L1 X-Ray Absorption near Edge Structure of Supported Pt Nanoparticles. *Top. Catal.* **2011**, *54* (5–7), 334–348. https://doi.org/10.1007/s11244-011-9662-5.

(50) Bjørgen, M.; Joensen, F.; Lillerud, K. P.; Olsbye, U.; Svelle, S. The Mechanisms of Ethene and Propene Formation from Methanol over High Silica H-ZSM-5 and H-Beta. *Catal. Today* **2009**, *142* (1–2), 90–97. https://doi.org/10.1016/j.cattod.2009.01.015.

(51) Bjørgen, M.; Svelle, S.; Joensen, F.; Nerlov, J.; Kolboe, S. Conversion of Methanol to Hydrocarbons

over Zeolite H-ZSM-5 : On the Origin of the Olefinic Species. **2007**, *249*, 195–207. https://doi.org/10.1016/j.jcat.2007.04.006.

(52) Svelle, S.; Joensen, F.; Nerlov, J.; Olsbye, U.; Lillerud, K. P.; Kolboe, S.; Bjørgen, M. Conversion of Methanol into Hydrocarbons over Zeolite H-ZSM-5: Ethene Formation Is Mechanistically Separated from the Formation of Higher Alkenes. *J. Am. Chem. Soc.* **2006**, *128* (46), 14770–14771. https://doi.org/10.1021/ja065810a.

(53) Corbetta, M.; Manenti, F.; Pirola, C.; Tsodikov, M. V; Chistyakov, A. V. Aromatization of Propane : Techno-Economic Analysis by Multiscale " Kinetics-to-Process " Simulation. *Comput. Chem. Eng.* **2014**, *71*, 457–466. https://doi.org/10.1016/j.compchemeng.2014.10.001.

For Table of Contents Use Only

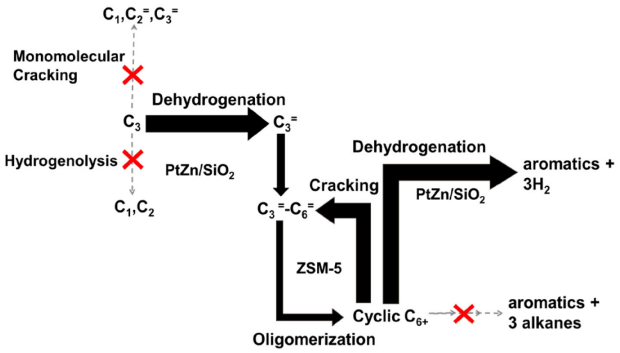


A molecular level understanding of the elementary steps in the reaction pathways improved formulation of catalyst compositions to give higher BTX yields with less methane